CURJ

WINTER 2008–09 vol. 9. no. 1
CALTECH UNDERGRADUATE RESEARCH JOURNAL

CURJ

Cs COMPUTER SCIENCE
Ce CHEMICAL ENGINEERING
Me MECHANICAL ENGINEERING
Ms MATERIALS SCIENCE
Bi BIOLOGY

CALTECH UNDERGRADUATE RESEARCH JOURNAL vol. 9. no. 1

from the editor

As we enter a new year, we should take a moment to reflect upon the events of last year. The year 2008 saw calamities from destructive earthquakes in China and Pakistan to the cyclone that devastated Burma. About two million people were newly infected with HIV in sub-Saharan Africa. With the rising unemployment rate and the falling economy, the year ended on an uncertain note.

However, there were also moments of peace and discovery. Transcending political differences, 11,028 athletes representing 204 nations gathered at Beijing for the summer Olympics. In research, we also saw a cure, albeit impractical, to HIV; the discovery of the fourth and final circuit element, the memresistor; and the first synthetically recreated bacterial genome modeled after Mycoplasma genitalium.

The most amazing thing about research is that, regardless of whether the times are difficult or easy, countless number of people of varying race, gender, background, and belief are working to understand the mysteries of the world and innovate solutions to the problems facing society. Just think – hundreds of years ago, people believed that earthquakes were divine repercussions of the gods. Now, researchers around the world are working to better understand and predict earthquakes, while engineers are developing structural designs that will better withstand the shaking. However, as this issue's interview will remind us, research is not limited to those wearing white laboratory coats and using pipettes; research is done in all areas, including education, environment, health, and economics. Research promises future solutions to the various problems facing society today.

In the Caltech Undergraduate Research Journal, we honor undergraduates and their passion for research by showcasing a variety of innovative research, whether it is developing improved methods of drug delivery, innovating new technologies to meet increasing energy demands, or improving the reliability and accuracy of information in publicly editable media. We are also proud to honor students from the Massachusetts Institute of Technology for the first time by reprinting an article from our sister journal, MURJ. More importantly, this journal honors you, the reader, as an informed member of society. The entire CURJ staff hopes that CURJ will inspire and rouse its readers to be passionate about the breakthroughs promised by research.

The new year brings new changes, a new president, and new areas of research. One thing is certain: the issues facing the world today underscore how important research and the innovations brought about by research are to both present and future generations. Enjoy CURJ, and continue supporting undergraduate research!

Best regards,

Joy Sheng

Co-editor-in-chief, 2008-2009

Interview with Professor Erik Snowberg Assistant Professor of Economics and Political Science

Photographs by Anna Malsberger

Erik Snowberg is an Assistant Professor of Economics and Political Science at the Caltech Division of Humanities and Social Sciences. He received a B.S. in Physics and Mathematics, with a minor in Economic, at MIT, and he received his PhD in Business from Stanford. His research interests include political economics, American politics, and behavioral economics. When he's not hard at work on his next paper, he likes to think about the paper he will write after that.

1. You received your undergraduate degrees in physics and mathematics at MIT, with a minor in economics. How did you become interested in economics and politics, and why did you choose to focus on economics and politics instead of physics?

I started out in physics because it's really exciting; I would roll the ball down the ramp into the coffee can and think, "This is so awesome! I can do something." Then I got to quantum physics my sophomore year, and it started to get abstract. By the time I got to quantum physics two, I was going, "What the hell is going on here?" So I lost interest in that.

Actually, my best friend in college lost interest in physics about the same time and is now a biologist at Stanford. Why I ended up in economics and politics and he ended up in biology, it was probably largely circumstantial. For me, there was this program at MIT that allowed you to spend the summer doing policy work in Washington D.C. So I interviewed for this program, and I lucked out and got in. That was when I was thrust into the political world.

2. You taught PS 126: Business, Public Policy, and Corruption Fall 2008. Why did you choose to teach it, and what was the class about?

I did my undergrad at MIT, and, like Caltech, you're required to take a certain number of humanities and social science classes. There was this feeling among the undergrads that the only reason the humanities and social sciences faculty existed was to socialize us. I think that trivializes a lot of the research that goes on both there and here, but on the other hand, being socialized is a really useful thing. So I wanted to teach a class where students had to make decisions with ambiguous data and discuss their solutions. How to get your voice heard, how to get your solutions across – these are skills that are super important, whether you are working in a lab group in graduate school, running your own lab, or working in a company.

So I adapted a class that we taught at Stanford and combined it with a class taught at Harvard. We took case studies of companies, where there are some data on the company and how it works, and had to think as a group about what the company should do next for a particular problem. Usually it was a company facing a problem of regulation or bad publicity, and the class was about the process of figuring out the best way to deal with the problem.

5. What are some of the similarities and differences between political science and physics?

With physics, somebody comes in and writes a model down on the board. They say, "We believe we have this model of the world, where if we put a force here, something is going to happen over there." But it's really just a model. It seems a lot like truth because there's a lot of experimental verification, and nobody ever says, "Well, what if F does not equal to m*a?" That's never on the table. The difference with political science and economics is that it quickly becomes apparent that the models aren't that good. There's less of a danger of that in physics. But physics and economics are both just models of the world. It just so happens that physics models predict a lot better.

I actually don't think that I learned how to become a scientist until I started taking social science classes because then you have to start thinking, "Am I doing science? Am I testing a proposition that I want to test?" Physics, chemistry, and biology, they're such closed systems that you can't really help but to do science. You don't even think about it: you apply these theorems, and you know they're true. In economics, there are theorems, but a lot of times the conditions aren't satisfied in the real world. You have to be more aware of the assumptions that go into the model, as opposed to something like physics, where you don't really think about what you're assuming about the world unless you're deep in the analysis. So it wasn't until I got into social sciences that I learned about the philosophy of science and how can you tell if you're testing a proposition or doing something circular.

6. You have published quite a few research papers. What did you find to be most interesting from your research?

The first paper I wrote was on how newspapers treated campaign finance. What we basically did was look at the five largest circulation newspapers and found every article in six years where they cited an amount of campaign funds - when the papers said "person X donated so much to candidate Y." I coded this data up, and just took an average. When individual contributions to candidates are reported, what was the average contribution amount? What is the actual average contribution amount to a candidate? What we found was that, in general, these things were off by an order of magnitude. It was a simple thing to show that newspapers were reporting there was much more money in politics than in reality. It was very easy to show, and nobody knew it before.

Then we did a survey to ask how much people thought it costs to run a typical House of Representatives campaign. The actual answer is about three hundred thousand dollars. The answer you get from the newspapers is about $1.3 million dollars. The interesting thing was that people who were college educated and most likely to read the newspaper a lot answered about $1.6 million dollars. When you asked people in the lowest education bracket, or people least likely to read the newspaper, they got it right - three hundred thousand dollars. We didn't show that this was caused by reading newspapers, but we showed that there was a correlation. It was so easy to do - you can ask a question, and you can get towards an answer – and this is exciting for me. And you don't need a ton of math to understand it.

7. What topics are you looking into for future research?

I'm starting some new projects and trying some new things. I'm very interested in getting more involved in looking at the way that religious organizations are involved in politics, and the economics of what makes people more or less likely to be members of religious organizations. That's a new direction for me, but I feel like there hasn't been much good research done in this area. In America, at least, these are incredibly important questions: where does the evangelical movement come from and just how politically powerful is it? I'm also continuing to work on prediction markets and some other research I started as a grad student about political economy in general, such as the role of parties and electoral competition in forming policy.

8. There's a lot of talk in the media right now about the state of economy and the ongoing recession. What is your opinion of the current financial crisis?

In general, I think one of the things that get underemphasized is the role of academia in how this financial crisis came about. To a very large extent, we've gotten a lot better at our models of our financial systems over the past, say, 50 years. That's generally a good thing, because it allows companies to figure out financial risks a lot better. But instead of having a whole bunch of models in the marketplace that get competed out in a Darwinian way, a lot of people just use whatever the academic researchers are doing and teaching in business school. Generally, the models are pretty good, but to the extent that these models have flaws, those flaws are going to show up all at once if everyone is thinking the same way. Everyone is going to be on the wrong side of some bet, and I think this is vey much what happened here.

We're doing such a good job of educating everybody in the same models that people aren't thinking enough for themselves. Business schools are all sort of uniform – they all try to be Harvard or Stanford, and the problem is that you're not bringing enough new ideas in. I'm just as guilty of this as anyone else; I based my class on those taught at Harvard and Stanford. A good business school should be trying to educate a lot of different people with a lot of different backgrounds in business so that they can go out in the marketplace and put forth different ideas that will be competed out. Because these people who end up in these top banks get trained in the same few business schools, and these business schools all try to be the same, there isn't much diversity.

Diversity is really important because otherwise everyone looks for the same information. Another example of where this happened was going into the Iraq war. There is a question of why we thought there were weapons of mass destruction in Iraq. Well, we had a lot of "independent" sources telling us that. It turns out that most of those sources were getting their information from one guy, code name Curveball. You get these problems where because you think twenty people tell you so, it must be true, but really there's only one person behind it all. Without independent chunks information, you're only going to have one answer. Unless you have other people with diverse ideas, you're going to end up all screwing up at the same time.

9. The traditional image of the ivory tower symbolizes the separation of scientists from the rest of the world. What do you think is the role for scientists in society?

I don't think there's anything that should separate scientists from anybody else in terms of trying to be good members of society and good citizens. But there is a question about how culpable should scientists be for the results of their discoveries. One extreme says you should hold scientists responsible, and the other extreme says you shouldn't because what you really want is for the scientist to explore everything and have someone else to make the determination of whether it's good or bad. I think I tend to agree with the latter – you shouldn't be locking scientists for trying to figure out how to clone things or any number of things that are ethically questionable. But as a scientist, you have to think, "Am I going to be comfortable if something I invented or thought of fell into the wrong hands or was used in the wrong way?"

"I think that as scientists, society usually won't tell you that you are doing something wrong. But you should be thinking if you're really comfortable with how your research could be used."

The bombing of Hiroshima and Nagasaki is a great example. Many of the scientists in the Manhattan Project were there because they didn't want Hitler to get the bomb. But Europe was won before we dropped atomic weapons on Japan, so at that point we knew Hitler wasn't getting the bomb. Only one scientist actually packed his bags and left the Manhattan Project at that point, a guy by the name of Joseph Rotblat, who went off to found an organization called Pugwash; he and Pugwash won the Nobel Peace Prize in 1995. Everybody else stayed on, but some of them got worried about using the weapon. There were these scientists who thought it was a bad idea, but they didn't do the one thing they could do, which was to stop working. They just wanted to lobby their politicians to do the right thing. That's a particular way to go about it and that's fine, but afterwards I think a lot of those people regretted it.

I think that as scientists, society usually won't tell you that you're doing something wrong. But you should be thinking if you're really comfortable with how your research could be used. If something is fuzzy, you have a lot of power to push the positive ways that you think the findings could be used, instead of the negative ways.

10. Do you have any advice for Caltech undergraduates?

I would say two things. There was a literature class I took at MIT where the professor was really adamant that we couldn't use what she called "dork analogies." If we were reading something in literature, we couldn't say this is just like a certain physics problem. But the way that people learn about the world is to relate it to something that they already understand, to say that this is kind of like that. Then you start to figure out the ways in which it's actually a little different from that. So my first piece of advice is: don't be shy about dork analogies. They're great.

The second piece – I remember being an undergrad as a pretty overwhelming thing, and the fact of the matter is, if you keep plugging away, you're going to make it. And the less you can worry about where you're going, the better. If you just do the things you enjoy, at the end of the day, at least you enjoyed yourself. If you do the things you think you should do, and you don't enjoy it, if you end up failing, then you didn't even enjoy yourself. I know everyone says it, but it's so true. Just do the things you enjoy. If you enjoy them, you're going to want to do more of them, and you're going to do it better, and you're ultimately going to succeed. Don't let some sense of where you should be going dictate what you're going to do. Just do what seems to be the most fun and be the best at doing it. If you really enjoy playing Pac-Man, just keep doing it – be the best at playing Pac-Man, there's nothing wrong with that.

Wikiganda: Propaganda Analysis

Identifying Through Text

Rishi Chandy
Mentors: K. Mani Chandy and Virgil Griffith

Launched in 2001, Wikipedia is now one of the largest collaborative digital encyclopedias in the world, with article quality similar to that of Britannica. Users can edit Wikipedia articles directly and view changes instantly, providing an incentive for contribution. Consequently, millions around the world turn to Wikipedia as a first reference for information about practically anything that might cross their minds.

However, the growth of such publicly accessible information does not come without risks. With few restrictions on article editing, Wikipedia relies on its users to recognize and correct content that fails to adhere to its editing standards, such as conflicts of interest (COI) and biased points-of-view. As such, people seeking to portray history from a prejudiced standpoint or to run misinformation campaigns could potentially run rampant, unchecked by any independent authority, and taint the neutral viewpoint of an otherwise excellent encyclopedic entry.

In 2007, Virgil Griffith released Wikiscanner, an online tool that allows users to trace anonymous Wikipedia edits back to the organization that owns the editor's IP address, thus exposing revisions made by that organization's employees. Wikiscanner became a sensation as several embarrassing edits from corporations became public and created minor public relations disasters.

Still, Wikiscanner independently is not able to determine if a Wikipedia revision contained propaganda; it merely identifies the source and relies on the user to judge the content. Here, we integrate Wikiscanner with recent research in opinion mining and sentiment analysis, which has provided new insight into the nature of emotion in text, especially in collaborative environments such as Wikipedia. This new tool, Wikiganda, uses text analysis and public data sources to pinpoint organizations that contribute possibly malicious propaganda to Wikipedia; Wikiganda aims to provide an effective platform to detect propaganda automatically. Wikiganda can be explored at http://www.wikiwatcher.com.

Categorizing Propaganda

Positive Propaganda, Negative Propaganda, and Vague Propaganda. Positive Propaganda occurs when an editor attempts to portray the subject of the article in a positive light by removing any negative criticism and adding excessive praise, while Negative Propaganda is the opposite. Vague Propaganda exhibits the properties of both Positive and Negative Propaganda.

In the example shown in Table 1, an editor from Exxon Mobil Corporation, according to IP2Location, a database of IP address owners, has added Positive Propaganda to the "Exxon Valdez Oil Spill" article. Casual users reading the article after this revision occurred would not see the text removed from the previous version, such as information about animal deaths, and therefore would assume that this was the only perspective on the subject. In addition, most users would not check the anonymous author's IP address and would fail to see the apparent conflict of interest, taking the biased information at face value.

Text as of 21:38 December 29, 2004	Text as of 22:03 December 29, 2004 Edited by 192.67.48.156 (Exxon Mobil Corp.)
Thousands of animals perished immediately, the best estimates are: 250,000 sea birds ... and billions of salmon and herring eggs... In the long term, declines have been observed in various marine populations, including stunted growth and indirect mortality increases in pink salmon populations...	Peer-reviewed studies conducted by hundreds of scientists have confirmed that there has been no long-term severe impact to the Prince William Sound ecosystem. Thousands of species in Prince William Sound were never affected by the spill in the first place... As an example, six of the largest salmon harvests in history were recorded in the decade immediately following the spill...

Table 1: An example of Positive Propaganda on Wikipedia for the "Exxon Valdez Oil Spill" article.

Identifying Propaganda

Wikiganda identifies the polarity, or the positive or negative subjectivity, of a given Wikipedia revision using sentiment analysis to approximate the author's feelings. From this information, Wikiganda's propaganda classifier can place the revision into one of the propaganda types mentioned above.

The Wikimedia Foundation provides a complete revision history of every article, which lists the time, editor, and text of each edit. By analyzing this information, Wikiganda scores each revision on a propaganda scale based on several metrics. In addition, the intuitive web interface allows the public to find propaganda on Wikipedia, searching by article or conflicting organization.

Setup

Since one of the secondary goals of Wikiganda was to connect editor IP addresses to organizations and geographic locations, all of the anonymous edits were extracted from the March 17, 2008 Wikipedia database using a Python script. Then, each revision was labeled with the organization or ISP that owned the editor's IP address, according to the IP2Location database.

The web interface allows users to specify opposing "teams" of organizations, such as Microsoft and Yahoo VS. Google, so that Wikiganda would display all articles that one or more "players" from each team had modified. To facilitate this, the labeled revision history was aggregated so that articles were grouped by organization name, thus reducing the time needed to perform the intersect query.

Article Controversy Indicators
of Revisions on Talk Page (+)
of Revisions (+)
of Unique Editors (-)

Table 2: +/- show controversy correlation. "Talk Page" refers to the article's discussion page.

Revisions-level Metrics
Vandalism
Sentiment Detection
WikiTrust values
Conflict of Interest

Table 3: Revision-level Metrics used as indicators for propaganda in Wikipedia revisions.

The web interface allows users to specify opposing "teams" of organizations, such as The respectable Microsoft and Yahoo VS. Google

The Propaganda Metrics

Article-level Metric

Previous research has established indicators (Table 2) to identify controversial articles in Wikipedia. Wikiganda uses Article Controversy as a metric because controversial subjects attract propaganda from opposing interests.

After extracting 2,385,595 unique article names from the revision history, the article-level statistics were calculated for each article based on the revision history database. These statistics, which are shown in the user interface, are used to compute Article Controversy when scoring individual revisions for propaganda.

Revision-level Metrics

The revision-level metrics operate by analyzing the diff and computing a Propaganda Score from 1 to 10. Several user-created automated processes on Wikipedia, such as ClueBot, use heuristics to detect and correct vandalism. Using those heuristics, Wikiganda detects vandalism common in some types of propaganda, such as obscenities and large deletions.

Wikiganda uses a polarity classifier based on a lexicon of over 20,000 words built from the Positive, Negative, PosAff, and NegAff categories from the General Inquirer word list and the prior polarity word list from Wiebe. Every word that is changed in a revision is matched against this lexicon.

Previous sentiment classification research has focused on collections of writings that are flat, such as movie reviews. In contrast, Wikipedia diffs show the words changed from the previous revision. Because of this, classical sentiment classification techniques cannot be applied directly to the diffs. To place the revision in one of the Propaganda Classes described above, Wikiganda computes the frequency of words added or deleted for each polarity,positive or negative. If the net positive change, or the difference between positive words added and positive words deleted, is greater than the net negative change, then the revision is labeled as Positive Propaganda. The reverse rule applies for Negative Propaganda. If the net positive change is equal to the net negative change, then it is considered Vague Propaganda.

Another important revision-level metric used in Wikiganda is WikiTrust. As part of the WikiTrust investigation into trust and content-driven author reputation in Wikipedia, researchers at the University of California Santa Cruz WikiLab have computed the trust values for revisions up to February 2007. The trust values indicate revision stability, or how long the changes of the revision lasted through the history of the article. Revisions that introduce flagrant propaganda can be unstable since users would recognize and correct them, so these trust values are a useful metric for revision-level propaganda.

The most blatant propaganda may originate from a conflict of interest, so Wikiganda also considers a Conflict of Interest Score. Daniel Erenrich has developed a system that flags revisions tainted by conflicts of interest. This depends on several factors, such as the connection between the article content and the organization that owns the editor's IP address. For example, a revision where a user from an Apple IP address edits the Wikipedia article for the iPhone would be flagged as a conflict of interest. Based on these factors, the system computes a Conflict of Interest Score.

	Predicted Not Propaganda	Predicted Propaganda	Sum
Not true propaganda	93	39	132
True propaganda	25	43	68
Sum	118	82	200

Table 4: Confusion Matrix for Propaganda Classifier. Overall, Wikiganda is 68% accurate.

Evaluation

Using a manually labeled test set of 200 randomly selected revisions, RapidMiner was used to train a decision tree for Wikiganda to score propaganda. The algorithm is implemented in PHP so that Wikiganda can follow the decision tree with input from the web interface.

After stratified ten-fold cross-validation, Wikiganda's propaganda classifier is found to be 68% accurate, with 52.439% Precision (true positive divided by sum of true positive and false positive) and 63.235% Recall (true positive rate). Always choosing the majority class, or "not propaganda," would only give 66% accuracy, so Wikiganda is slightly more accurate.

By combining the Propaganda Classifier with the work of Virgil Griffith and other collaborators in Professor Chandy's Infospheres Laboratory, Wikiganda can approximately identify propaganda and conflicts of interest on Wikipedia.

Future Directions

These methods can be applied to other sources of user-generated content in addition to Wikipedia. In the future, this research could include a deeper analysis of the article revision history to trace the evolution of specific misinformation. Also, it may be possible to automatically determine an organization's stance on issues based on its edits to related Wikipedia articles.

Further Reading

1. Adler, B., Chatterjee, K., de Alfaro, L., Faella, M., Pye, I., Raman, V. Assigning Trust to Wikipedia Content. WikiSym 2008: International Symposium on Wikis (2008) at http://www.soe.ucsc.edu/~luca/papers/08/wikisym08-trust.html

2. Erenrich, D. Wikiscanner: Automated Conflict of Interest Detection of Anonymous Wikipedia Edits. (2008).

3. Stone, P. J., Dunphy, D. C., Smith, M. S., Ogilvie, D. M. 1966. The General Inquirer: A Computer Approach to Content Analysis. MIT Press, Cambridge, MA.

4. Vuong, B. et al. On Ranking Controversies in Wikipedia: Models and Evaluation. Proceedings of the international conference on Web search and web data mining 171-182 (2008).

5. Wilson, T., Wiebe, J., Hoffmann, P. Recognizing Contextual Polarity in Phrase-Level Sentiment Analysis. Proceedings of Human Language Technology Conference and Conference on Empirical Methods in Natural Language Processing, 347-354 (2005).

Acknowledgements

Rishi Chandy is a sophomore in Computer Science at Caltech. He would like the thank Professor K. Mani Chandy and Virgil Griffith for their valuable mentorship; B. Thomas Adler, Jason Benterou, Krishnendu Chatterjee, Luca de Alfaro, Ian Pye, and Vishwanath Raman for access to the WikiTrust data; and Daniel Erenrich for access to the Conflict of Interest data. He would also like thank Charles Slamar and Kristen Vogen of J. Edward Richter Memorial Funds for their generous donation and sponsorship.

"It may be possible to automatically determine an organization's stance on minor issues based on its edits to related Wikipedia articles."

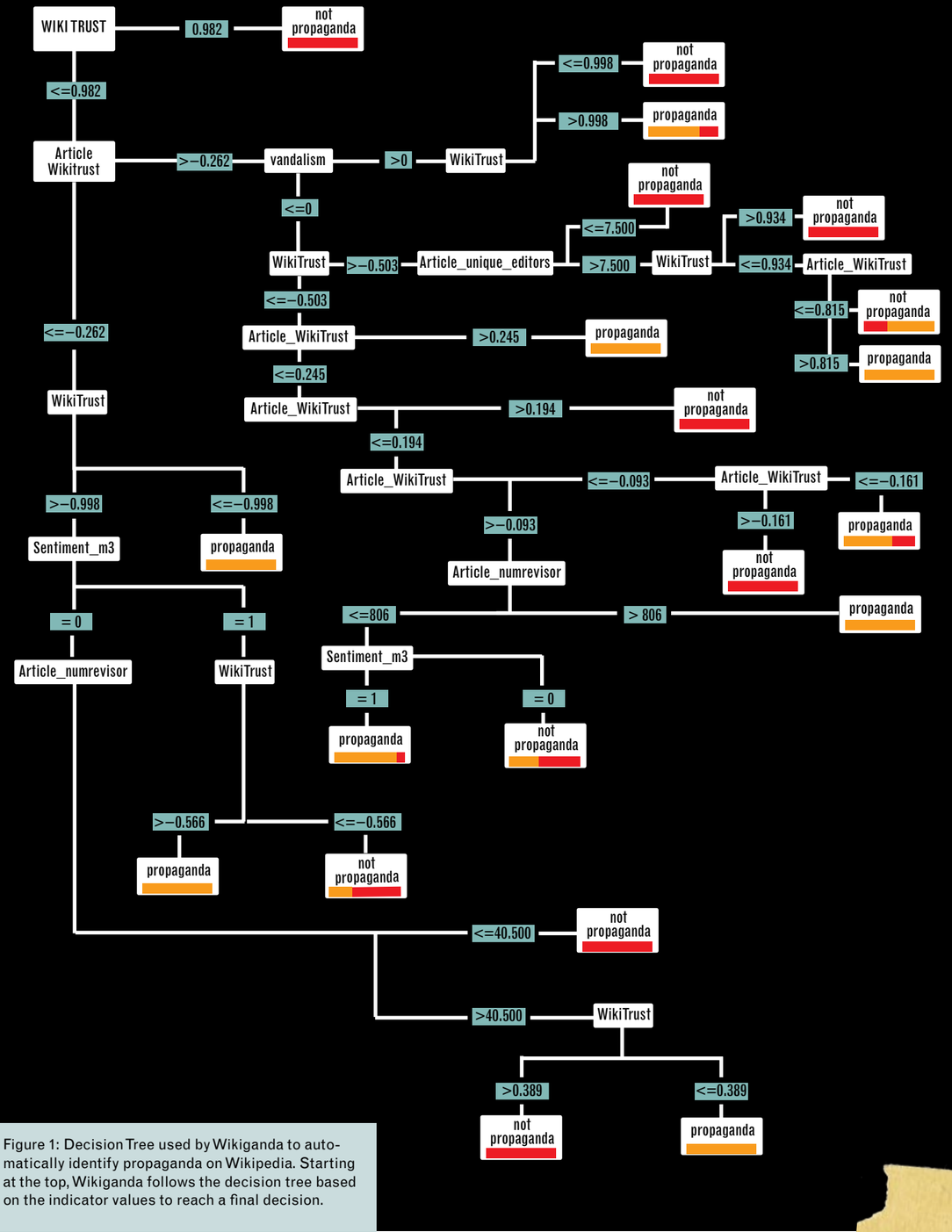

Figure 1: Decision Tree used by Wikiganda to automatically identify propaganda on Wikipedia. Starting at the top, Wikiganda follows the decision tree based on the indicator values to reach a final decision.

Let the specialist do the job

Shuyi Ma
Mentor: Frances H. Arnold
Co-Mentor: Sabine Bastian

Drug development is a highly selective process; only a handful out of thousands of compounds reaches the hands of the public. The discovery of potential drug compounds often involves regioselective replacement, or the modification of a chemical scaffold by replacing the side groups of a scaffold molecule. Functional side groups of the scaffold molecule can be exchanged to acquire desired chemical properties of a potential drug, but switching the side groups requires breaking and making bonds that are quite strong. Synthetic chemical approaches to impose these changes regioselectively usually involve multiple steps, harsh reaction conditions, and hosts of assisting and protective molecules. The net reaction is thus quite difficult and costly, especially in an industrial setting.

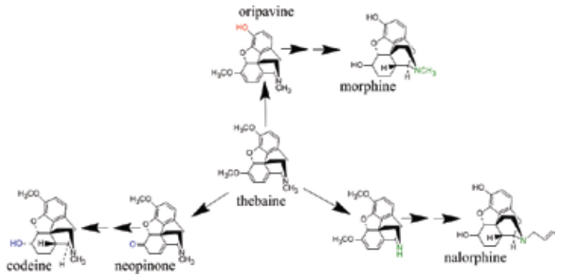

Figure 1 The drug compound thebaine and its related products[2]. This scheme illustrates how new pharmaceutical products can be readily accessed by exchanging functional groups on the scaffold of a single structure.

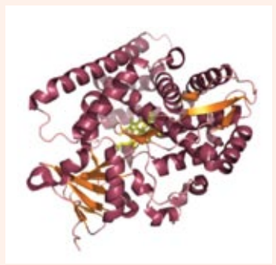

Figure 2 Crystal structure of the heme domain of cytochrome P450BM3.

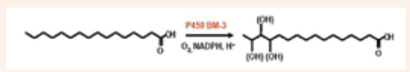

Figure 3 Hydroxylation reaction of fatty acids catalyzed by P450BM3.

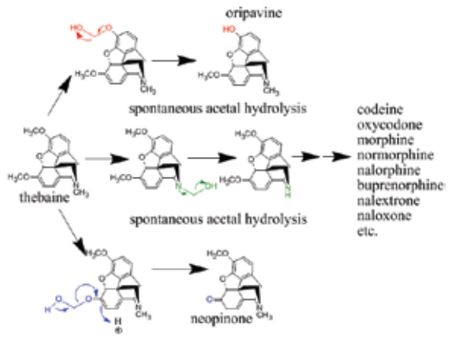

Figure 4: Proposed demethylation reactions of interest. The reaction pathway highlighted in blue which yields neopinone cannot be accomplished using traditional synthetic chemistry methods

Our particular scaffold of interest is thebaine, a modified benzyltetrahydroisoquinoline alkaloid related to morphine (Figure 1). This powerful nervous system stimulant is a precursor to several analgesics including codeine, and it has several groups that can be potentially modified, making it a strong drug engineering candidate. As expected, thebaine is difficult for synthetic chemists to adapt regioselectively; we examined the feasibility of applying an enzyme as a biological catalyst to modify thebaine.

Enzymes can catalyze selective functional group replacement reactions at ambient conditions with higher frequency and greater selectivity than synthetic catalysts. Our group is investigating the potential use of these catalysts from nature, which generally operate at much milder conditions, for regioselective reactions. Specifically, we chose to engineer the enzyme cytochrome P450BM3 (CYP102A1) from *Bacillus megaterium* (Figure 2) to catalyze our desired reaction. Cytochrome P450BM3 can catalyze reactions on its natural substrate at room temperature and pressure with high activity.

Why Train Cytochrome P450BM3?

The proposed benzyltetrahydroisoquinoline biosynthetic pathway utilizes a number of mammalian cytochrome P450-catalyzed steps to make morphine and codeine from thebaine, but these enzymes are unsuitable for protein engineering efforts as they are multi-component systems that are difficult to express in heterologous hosts like *Escherichia coli*. We have therefore chosen to apply methodologies of protein engineering to cytochrome P450BM3 to access our desired regioselective functions: namely, to catalyze regioselective demethylation of thebaine by hydroxylating a desired methyl hydrogen. P450BM3 is a good starting point; it is straightforward to engineer since it is soluble and is readily expressed in *E. coli*. Moreover, P450BM3 is an ideal catalyst as it exhibits high hydroxylation rates on preferred substrates like fatty acids (Figure 3), and all of the machinery required for catalysis—both the monooxygenase- and the reductase-domains—is included on a single polypeptide chain. P450BM3 cannot be immediately applied to catalyze the demethylation of thebaine because thebaine differs substantially in structure and in its physical properties from the natural substrates of P450BM3, fatty acids.

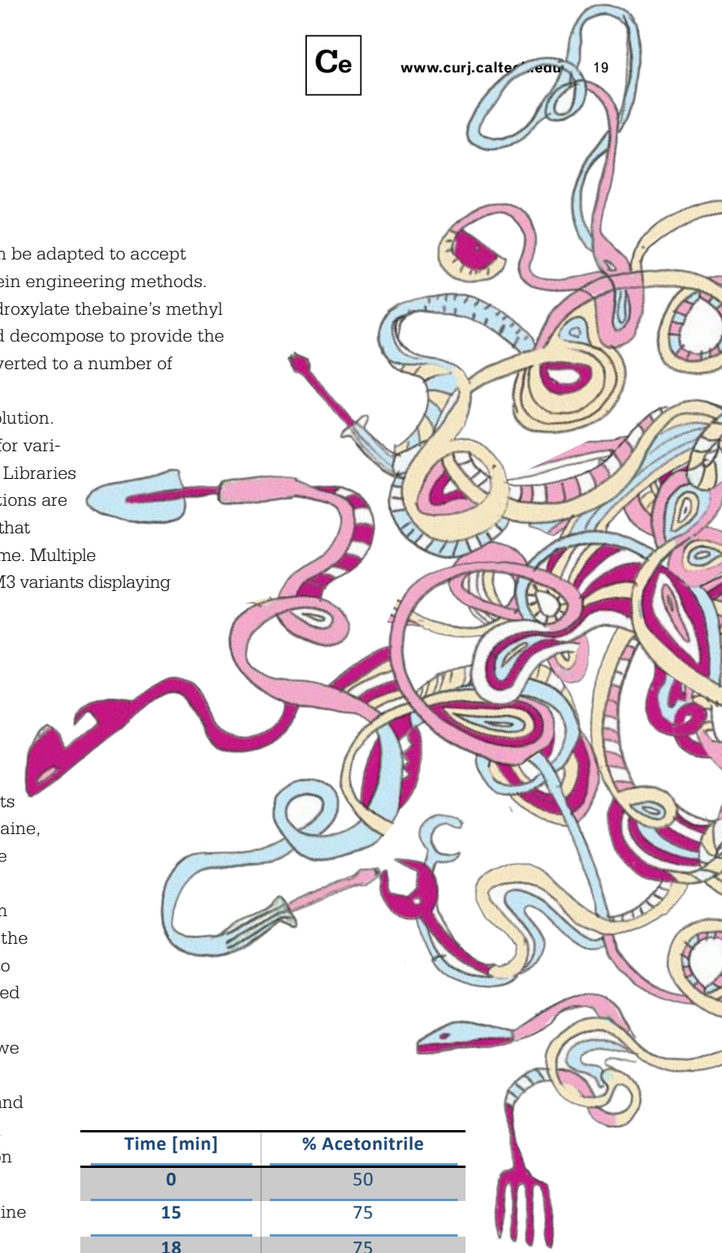

However, numerous studies have shown that P450BM3 can be adapted to accept substrates with substantially different properties by protein engineering methods. By engineering the substrate specificity of P450BM3 to hydroxylate thebaine's methyl groups, we hoped to generate intermediates which would decompose to provide the demethylated products (Figure 1) that can be readily converted to a number of important alkaloids (Figure 4).

One method of protein engineering is by directed evolution. Mutations are randomly introduced into the gene coding for variants of P450BM3 by error-prone polymerase chain reaction. Libraries of P450BM3 variants harboring a multitude of diverse mutations are generated. These libraries are then screened for candidates that exhibit traits which most closely resemble the desired outcome. Multiple iterations of mutagenesis and screening should yield P450BM3 variants displaying incrementally favorable traits.

Setting Conditions to Measure Our Product

In order to be able to distinguish between thebaine and its potentially demethylated products (*N*-demethylated thebaine, and *O*-demethylated thebaine), we configured the reverse phase high performance liquid chromatography (HPLC) flow profile of the liquid phase to maximize the separation between elution peaks of each thebaine derivative. With the peaks sufficiently separated, we can use the HPLC data to identify the type and calculate the amount of demethylated product is catalyzed by a given variant of P450BM3.

After experimenting with various HPLC conditions, we deduced that maximal separation of peaks was obtained using a 4.6 x 150 mm, 5µm-particle, Atlantis T3 column and a gradient of acetonitrile with 0.1% trifluoroacetic acid in water (Table 1). Although we obtained baseline separation of the thebaine and the demethylated product peaks, the *N*-demethylated thebaine and the *O*-demethylated thebaine peaks were too close together for baseline separation.

Time [min]	% Acetonitrile
0	50
15	75
18	75
18.01	50
20	50

Table 1: HPLC flow conditions. This profile yielded the best separation between the standards (thebaine, *N*-demethylated thebaine, and *O*-demethylated thebaine). Flow rate was 0.4 mL/min.

Finding the right starting place

The first step of directed evolution involves finding a promising parent enzyme that delivers sufficient catalytic activity to enable a colorimetric screen. To find the parent, we grew and expressed a compilation library consisting of P450BM3 variants generated by an algorithm which targets mutations on active site residues most likely to generate sequence diversity while maintaining an active fold. We screened variants of the compilation library that had previously demonstrated slight activity on thebaine. We assessed protein concentrations extracted from *E. coli* cells with a carbon monoxide (CO) binding assay, which operates on the principle that the reduced form of P450BM3 turns red in the presence of CO binding to its catalytic heme; this can be detected by a spectrophotometer. We screened the variants for thebaine hydroxylation activity with a colorimetric assay involving purpald, which reacts with the formaldehyde side-product of the desired reaction to form a purple compound that can be visually detected (Figure 5). Our screening results, confirmed by HPLC, yielded variants D6 and A11 as the most promising candidates from which to further engineer the desired enzymes. Sequencing results showed that the two parents contained a total of six mutations from wild-type P450BM3 in the active site of the enzyme (Table 2).

Variant D6 was selected for catalyzing reactions on both the methyl amine group and the methoxy groups of thebaine with a total turnover number of 27 (Figure 6a), and variant A11 was selected for selectively catalyzing reactions on the methoxy groups with a total turnover number of 17 (Figure 6b). Further characterization by 1H NMR of the extracted product of a bioconversion using D6 showed that the major product catalyzed was the *N*-demethylated compound.

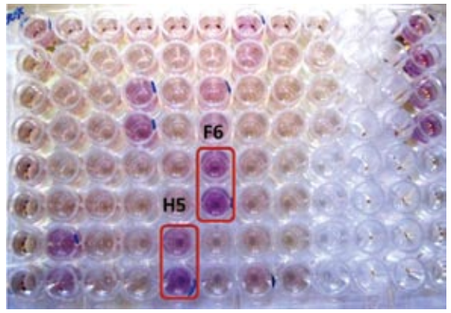

Figure 5 Rescreen results of promising D6 library variants tested in duplicate with purpald colorimetric assay. The red squares highlight the most active variants as evident by the darkest color: H5 and F6.

Amino acid position:	75	82	87	181	188	330
Wild-type	L	A	F	L	L	A
D6	**F**	**A**	A	F	W	**V**
A11	**L**	**S**	A	F	W	**A**

Table 2 Sequencing data shown as amino acid residues for the selected parents D6 and A11 compared to wild-type P450BM3. Each of these residues reside within the active site of the enzyme. The parents differ from each other by three amino acid substitutions (bolded).

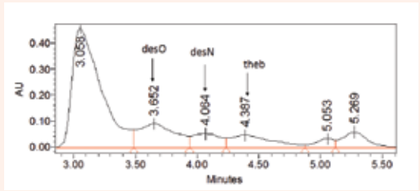

Figure 6a: HPLC absorbance peak chromatogram taken at 254 nm of 1 mL bioconversion product catalyzed by 1 µM of D6. Co-injection data (not shown) indicated that the peaks at 3.652 minutes and 4.064 minutes belong to the *O*-demethylated and *N*-demethylated product, respectively.

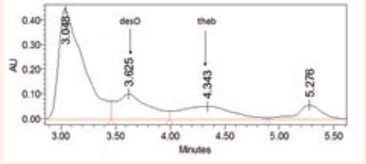

Figure 6b: HPLC absorbance peak chromatogram taken at 254 nm of 1 mL bioconversion product catalyzed by 1 µM of A11. Co-injection data (not shown) indicate that the peak at 3.625 minutes belongs to an *O*-demethylated product.

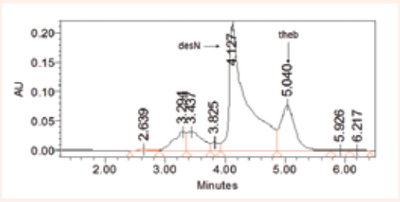

Figure 7a: HPLC absorbance peak chromatogram taken at 285.4 nm of 1 mL bioconversion product catalyzed by 1 µM H5. The largest elution peak at 4.127 minutes corresponds to the product demethylated at the methyl amine group (desN).

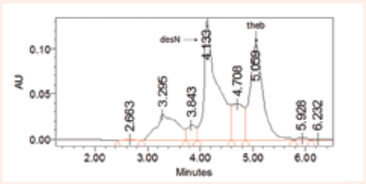

Figure 7b: HPLC absorbance peak chromatogram taken at 285.4 nm of 1 mL bioconversion product catalyzed by 1 µM F6. The elution peak at 4.133 minutes corresponds to the product demethylated at the methyl amine group (desN), and the peak at 4.708 corresponds to thebaine.

How we started training the specialist …

Once we selected promising parents, we extracted the plasmid carrying the gene coding for the enzymes as a template for random mutagenesis in the next step of directed evolution. A classic approach to introduce mutations randomly is error-prone polymerase chain reaction (epPCR), which involves replication of DNA using a polymerase chain reaction under conditions that allow for a regulated number of introduced mutations. We used *Taq* polymerase and controlled the mutation rate by varying the concentration of $MnCl_2$ in the 300 µL reaction mixture (higher concentrations of $MnCl_2$ yield higher mutation rates). The fractions of the 300 nM $MnCl_2$ variants in the D6 and A11 libraries that folded into the active conformation of a P450BM3 were comparable to the desired 50%, which is optimal for constructing a library that yields sufficient sequence diversity while retaining a high fraction of folded variants.

We ligated the resulting fragments of DNA into an *E. coli* expression vector that provides ampicillin resistance, and we transformed *E. coli* cells with the resulting plasmid by electroporation. We grew the cells and expressed 3,000 of the variant proteins for screening by the purpald colorimetric assay.

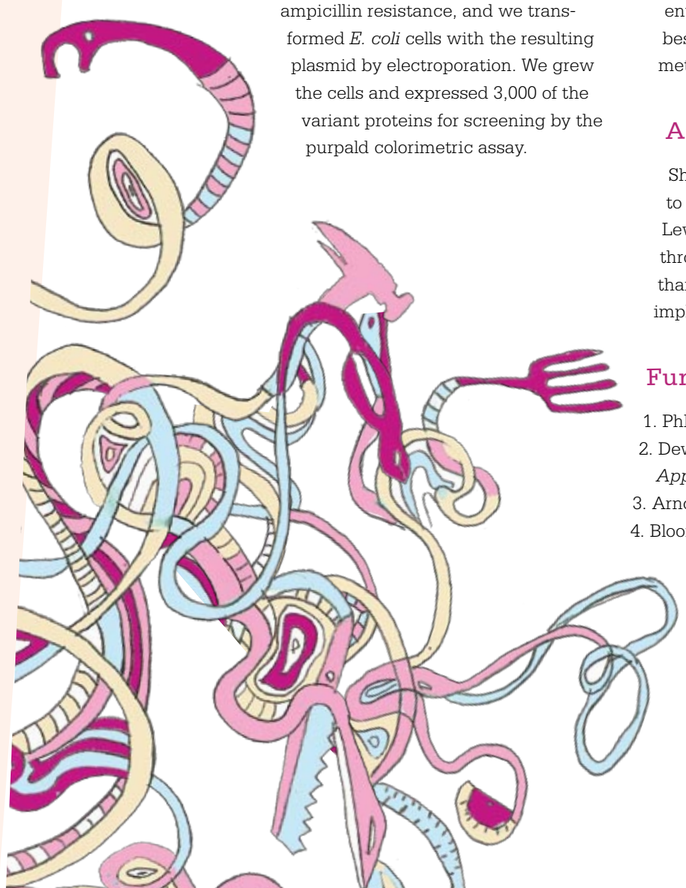

The best variants of the screen (H5 and F6 in Figure 5) were expressed, purified and further characterized. Sequencing results showed that H5 had accrued one mutation (Q37R), and F6 had accrued three (S65T, K241N, and T365I). Further analysis with HPLC demonstrated that the two variants exhibited improved demethylation activity at the methyl amine group. Based on the HPLC data, we found that H5 yielded 420 total turnovers (TTN) (Figure 7a), and F6 yielded 246 TTN (Figure 7b)

… and how training will continue.

Over the course of these experiments, we applied directed evolution toward engineering cytochrome P450BM3 for demethylation of thebaine. We have engineered two variants of P450BM3 with mutations inside and outside the active site that display significant demethylation activity on thebaine's methyl amine functional group. Future work will entail improved characterization of the activity of the current best variants and will also target demethylation at thebaine's methoxy groups.

Acknowlegements

Shuyi Ma is a senior in chemical engineering. She would like to thank Prof. Frances Arnold, Dr. Sabine Bastian, and Dr. Jared Lewis for their advice, insights, and continued encouragement throughout the duration of this project. She would also like to thank to Dr. Andrea Rentmeister and Mike Chen for help with implementation of some laboratory techniques.

Further Reading

1. PhRMA, "Pharmaceutical Industry Profile 2008"
2. Dewick, P. M., *Medicinal Natural Products; A Biosynthetic Approach*. (John Wiley and Sons, LTD., 2001)
3. Arnold, F. H., *Chemical Engineering Science* **51** (23), 5091 (1996).
4. Bloom, J. D. et al., *Curr Opin Struct Biol* **15** (4), 447 (2005).

Tapping Fluctuating Wind for Energy in an Urban Environment

Author: **Fei Yang**
School: California Institute of Technology

Mentor: **John O. Dabiri**
School: California Institute of Technology

Generation of power from alternative, sustainable energy resources is currently a high focus area of research. One somewhat overlooked area of sustainable energy is wind power. While wind power was developed earlier than many other renewable methods of energy production, its potential still has not been fully utilized. Current wind harvesting technology primarily relies on extracting energy from continuous wind. Therefore, only a limited range of wind velocity and conditions can be utilized to generate electricity. Currently, large or medium-scale wind-driven generators must be constructed in nearly unobstructed terrains with sustained, steady wind. However, potential from fluctuating wind, especially in urban environments, has yet to be fully utilized. Here the central question is if this fluctuating wind can provide a reliable source of energy.

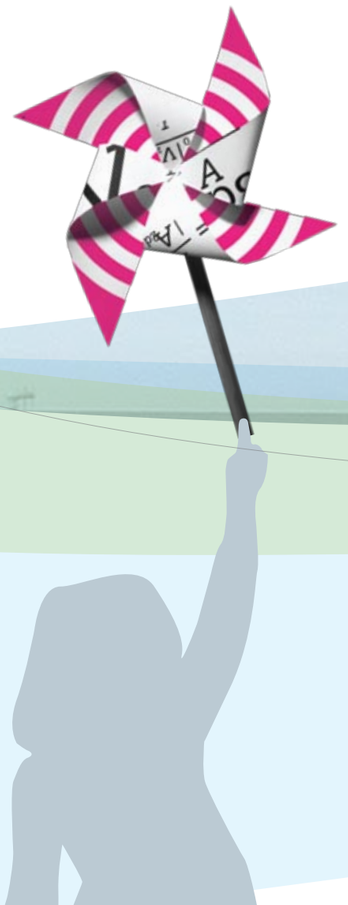

Theoretical Background

Previous work[3] has shown that the total power P_{ad} that can be extracted from wind characterized by velocity vector $V_{3d} = V_u + V_v + V_w$, air density, and traveling through an area parallel to can be approximated by

$$P_{ad} = \frac{1}{2}\rho A_{3d} \cdot V_{3d} |V_{3d}|^2 = \frac{1}{2}\rho |A_{3d}| |V_{3d}|^3 \quad (1)$$

For wind with velocity vector $V_{2d} = V_u + V_v$ (the horizontal projection of V_{3d}), the total power P_{2d} that can be extracted through an area A_{2d} perpendicular to the horizontal plane can be expressed as

$$P_{2d} = \frac{1}{2}\rho A_{2d} \cdot V_{2d} |V_{3d}|^2 = \frac{1}{2}\rho |A_{2d}| |V_{2d}| |V_{3d}|^2 \quad (2)$$

Therefore, the concept of power flux can be defined as power of wind flowing through a unit of area and can be expressed mathematically as,

$$\Phi_{3d} = \frac{P_{ad}}{|A_{2d}|} = \frac{1}{2}\rho |V_{3d}|^3 \text{ and } \Phi_{2d} = \frac{P_{2d}}{|A_{2d}|} = \frac{1}{2}\rho |V_{2d}| |V_{3d}|^2 \quad (3)$$

Previous work[3] has also shown that the maximum fraction of power in the wind that can be extracted from ideal wind turbines is 59.3%. However, because the power limitation is deduced from the application of simple momentum theory on steady, continuous wind, it may not be applicable to power extraction of unsteady, fluctuating wind. Furthermore, we attempt to study the total kinetic energy available in wind, ignoring technological limitations involved with extraction of wind energy.

We use three factors to quantitatively indicate the degree of fluctuations in wind energy: energy pattern factor (EPF), spatial energy pattern factor (SEPF), and total energy pattern factor (TEPF).

Consider a wind velocity vector $V_{3d} = V_u + V_v + V_w$ and its projection on the horizontal plane $V_{2d} = V_u + V_v$. The energy pattern factor of V_{2d} through the area A_{2d}, which is parallel to V_{2d}, over time T is defined as

$$K_6^{2d} = \frac{\int_0^T |V_{zd}| |V_{3d}|^2 dt}{T\left(\frac{\int_0^T |V_{zd}|}{T}\right)\left(\frac{\int_0^T |V_{3d}|}{T}\right)^2} \quad (4)$$

The numerator takes into account the energy available in V_{2d} through the time period T. The denominator approximates the total energy available in V_{2d} using mean speed. Previous work[3] has shown that energy pattern factor K_e is inversely proportional to the mean velocity and approaches one as the temporal velocity fluctuations decrease. Because current horizontal or vertical axis wind turbines are designed to extract energy from steady, two-dimensional wind with a high mean velocity, energy potential lost from wind fluctuations is insignificant compared to the total energy extracted. However, in an urban environment, where mean wind speed is low and fluctuations are common, we use EPF to determine the degree of wind speed fluctuations and the factor of energy potential that can be gained from capturing wind speed fluctuations.

If we assume $\overline{V_{3d}} = \frac{\int_0 |V_{3d}| dt}{T}$, $\overline{V_{2d}} = \frac{\int_0 |V_{zd}| dt}{T}$, and each velocity vector flows through an area of the same magnitude, where $|A_{2d}| = |A_{3d}|$, $A_{2d} \| V_{2d}$, and $A_{3d} \| V_{3d}$, then the spatial energy pattern factor of V_{2d} can be defined as

$$K_3^{2d} = \frac{\frac{1}{2}\rho |A_{3d}| (\bar{\bar{V}}_{3d})^3}{\frac{1}{2}\rho |A_{zd}| (\bar{\bar{V}}_{zd})(\bar{\bar{V}}_{zd})^2} = \frac{\bar{\bar{V}}_{3d}}{\bar{\bar{V}}_{2d}} \quad (5)$$

Because the numerator and the denominator approximate the energy available in V_{3d} and V_{2d}, respectively, by using the mean wind speed, this does not take into account the energy potential in fluctuations of wind. Current horizontal axis wind turbines are designed to capture wind energy in the horizontal plane. Therefore, they are specifically located where the vertical component of wind is negligible. However, in an urban environment, where buildings often force air to travel upward, the vertical component of wind velocity becomes significant. SEPF is a useful tool to indicate the degree of wind directional fluctuations and the factor of energy that can be gained from capturing all spatial components of wind. The TEPF of V_{2d} can then be defined as

$$K_t^{2d} = K_3^{2d} * K_e^{3d}, \text{where } K_e^{3d} = \frac{\int_0^T |V_{3d}|^3 dt}{T\left(\frac{\int_0^T |V_{3d}|}{T}\right)^3} \quad (6)$$

The denominator takes into account all the energy available in V_{3d} throughout the period T, while the numerator approximates the energy available in V_{2d}, discounting the effect of fluctuations. Therefore, TEPF simply indicates the total factor of energy that can be gained by capturing speed and directional fluctuations.

Figure 1. Velocity duration curves of a) Thomas, b) Millikan, and c) Baxter,. Linear spline curve fitting process is used for all datasets.

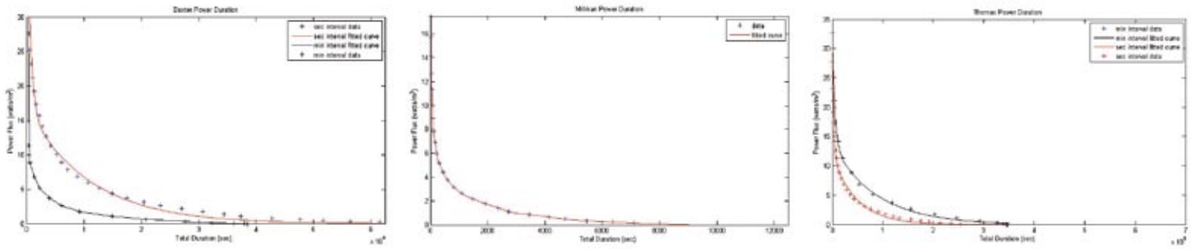

(a) (b) (c)

Figure 2. Power duration curves for a) Baxter, exponential curve fitting procedure is used, b) Thomas, exponential curve fitting procedure is used, and c) Millikan, linear spine curve fitting procedure is used

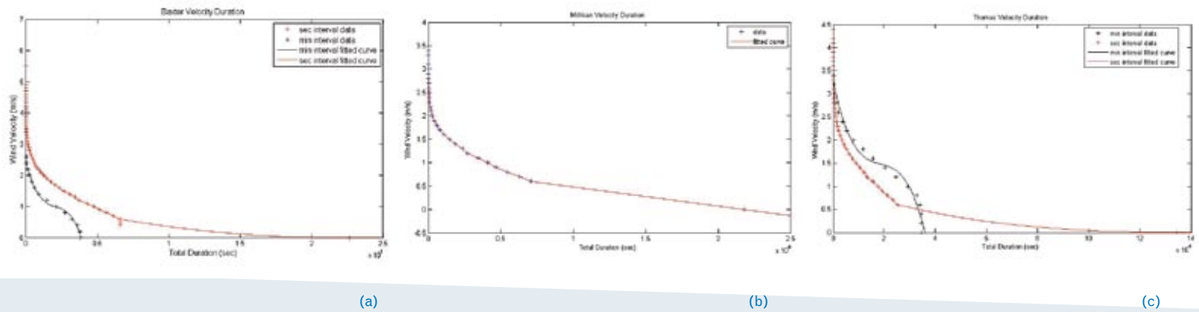

(a) (b) (c)

Speed Fluctuations

In the first part of our study, the fluctuations of wind speed were investigated. Wind speed was measured and recorded at three locations on Caltech Campus: the roof of Baxter (BAX), the Thomas radio tower (TMS), and the Millikan Bridge (MLK). Two types of anemometers, which are able to measure and record wind speed under different specifications, were used. Taylor Precision Instrument anemometers measured the average wind speed (each minute), and Windspeed anemometers measured the instantaneous wind speed (each second). Both anemometers recorded wind speed with 0.1m/s resolution. One Windspeed and one Taylor anemometers were mounted on Baxter and Thomas, while one Windspeed anemometer was used at Millikan. Five datasets were generated: minute interval Baxter, second interval Baxter, minute interval Thomas, second interval Thomas, and second interval Millikan.

In this study, wind speed data is analyzed and displayed as a velocity duration curve. Velocity duration curves plot the range of wind speed against the duration in time for which the speed equals or exceeds each particular value. Figure 1 indicates the velocity duration curves for each site. These curves lack wind speed data between 0m/s to 0.5m/s due to instrument limitations.

Figure 2 shows the power duration curve for the same datasets. A power duration curve plots the range of power flux against the duration of time for which power flux exceeds or equals to each particular value. Power duration curves were calculated from standard air density and wind speed data according to formula (3). The shape of each power duration curves reflects the nature of wind speed of a particular site. If the curves hug the axis closely, then most of potential is available from steady wind speed. On the other hand, if the curves rise gently as total duration decreases, then a significant amount of energy may be available from fluctuating, high wind speed. Moreover, the area under each power duration curve indicates the projected total energy available at each location.

Dataset	Air Density (kg/m^3)	Mean Wind Speed (m/s)	Total Energy (J/m^2)	Average Power Flux ($watts/m^2$)		Energy Pattern Factor (K_e)
				No Fluctuations	Fluctuations	
Minute Interval Baxter	1.29	1.1±0.1	56600±12400	0.8±0.3	1.5±0.3	1.8± 0.8
Second Interval Baxter	1.29	0.6±0.2	207500±38500	0.1±0.1	0.9±0.2	8.1±4.4
Minute Interval Thomas	1.29	1.6±0.2	126900±23200	2.6±0.5	3.7±0.7	1.4±0.6
Second Interval Thomas	1.29	0.4±0.4	63800±24600	0.04	0.5±0.2	11.0±9.6
Second Interval Millikan	1.29	0.6±0.2	10200± 3500	0.1±0.2	0.5±0.1	4.2±2.8

Table 1. Speed and potential energy of wind observed at 1) Baxter, 2) Thomas, and 3) Millikan. Because air density was not measured at each location, it was assumed to be 1.29 kg/m^3, the standard air density. Mean speed is the area under the velocity duration curves over the total observation time. Total energy collected is the integral of each power duration curve. Power flux represents the total power of wind for a given windswept area.

	Average time needed to charge a laptop battery (hr)		Amount of time one compact fluorescent light bulb can be powered by wind energy collected in day (hr)		Percentage of annual household energy consumption provided by wind	
	No Fluctuations	Fluctuations	No Fluctuations	Fluctuations	No Fluctuations	Fluctuations
Minute Interval Baxter	80±25	45±12	1.8±0.6	3.2±0.7	(3.1±1.0)%	(5.6±1.2)%
Second Interval Baxter	580±310	72±12	0.3±0.1	2.0±0.4	(0.4±0.3)%	(3.5±0.7)%
Minute Interval Thomas	26±5	18±3	5.6±1.1	8.0±1.5	(9.8±2.0)%	(13.9±2.5)%
Second Interval Thomas	1600±1300	140±39	0.1±0.1	1.0±0.4	(0.2±0.1)%	(1.8±0.7)%
Second Interval Millikan	520±320	140±36	0.3±0.2	1.0±0.4	(0.5±0.4)%	(1.8±0.6)%

Table 2. a) Typical energy capacity of laptop battery: 66Whr vs. power through a windswept area of 1m^2. b) Average power consumption of compact fluorescent light bulbs: 11watts vs. energy through a windswept area of 1 m^2 in a day. c) Average energy used by US household per year: 8,900kWh vs. energy through a windswept area of 38.5 m^2 in a year.

Table 1 shows mean wind speed, total energy, average power flux, and energy pattern factors for each dataset. A high value of K_e, above 2, indicates that a considerable increase in power potential would occur if the speed fluctuations of wind at those locations were harvested. Therefore, at sites characterized by high K_e values, significant increase in power flux from steady wind speed to fluctuating wind speed can be seen in Table 1. A low factor of K_e indicates the wind speed is fairly steady, and any additional power gained from capturing fluctuations is insignificant. EPF indicates not only the nature of wind speed fluctuations at a certain location, but more importantly, the magnitude of energy potential to be gained from capturing speed fluctuations.

Table 2 analyzes various power consumption models with projected power output for each dataset. This clearly demonstrates that the power potential of wind at each location is effectively increased by a factor of K_e if the potential of speed fluctuations is fully utilized. However, mean wind speed at each location is simply too low for wind to be a significant source of energy, even if power potentials of fluctuations are fully harnessed.

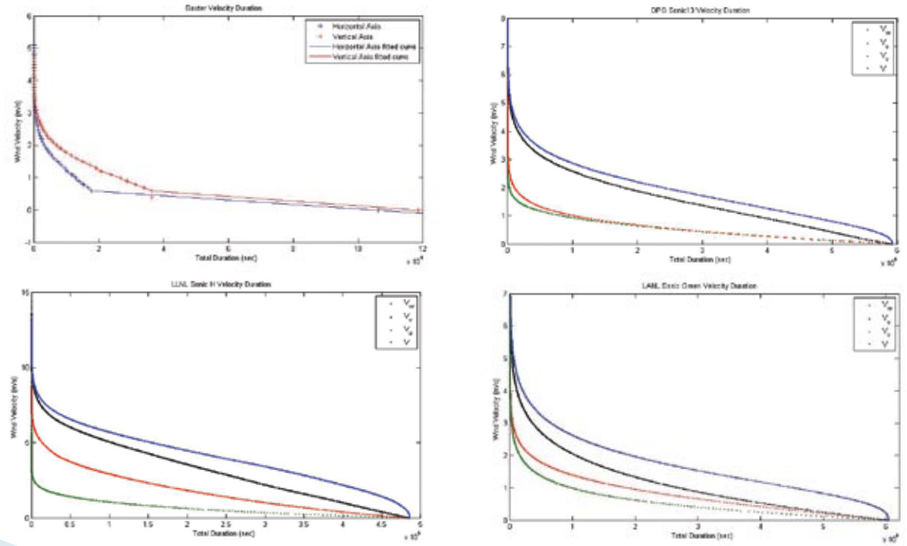

Figure 3. Velocity duration curves for a) LLNL_sonicH, b) Baxter, c) DPG_sonic13, d) LANL_sonicgreen. Linear spline curve fitting procedure is used for all datasets. In the velocity duration curve for Baxter, velocity data measured by horizontal and vertical axis anemometers are displayed together on one graph. For JUS datasets, individual components V_v, V_w, V_u, and the resultant velocity V, are displayed together on one velocity duration graph. The graphs indicate that wind has a dominant direction of travel at each site during the observation period; however, it also fluctuates more spatially at some sites than others.

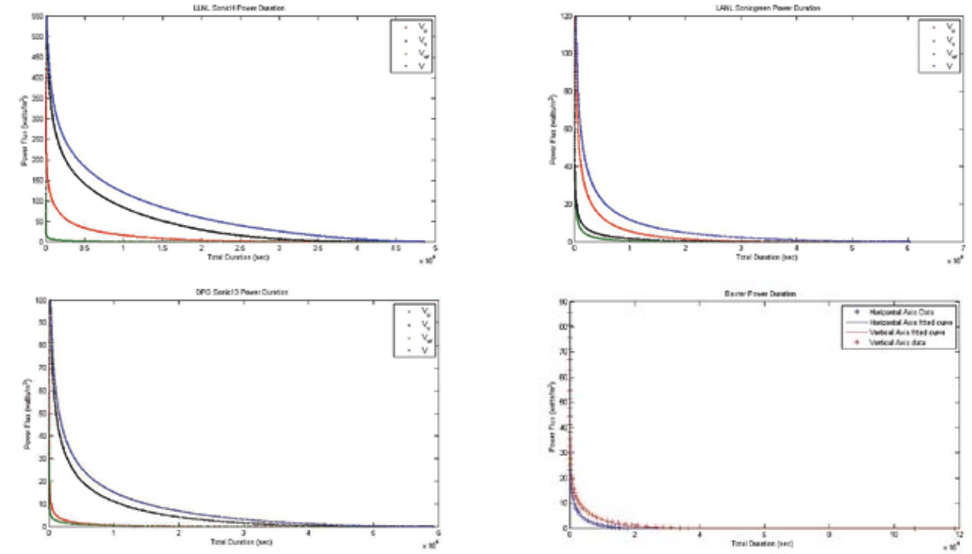

Figure 4. Power duration curves for a) Baxter (using exponential curve fitting procedure) b) DPG_sonic13, c) LANL_sonicgreen, d) LLNL_sonicH. Note linear spline curve fitting procedure is used for all JUS 2003 datasets.

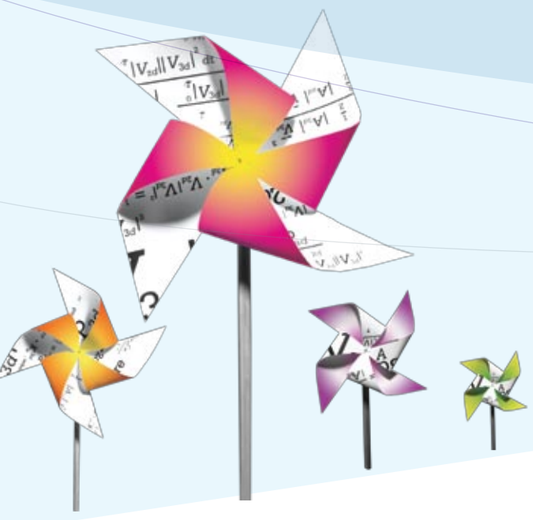

Directional Fluctuations

In the second part of our study, the effect of directional fluctuations is studied using data collected at Baxter and from the database of Joint Urban Study (JUS) 2003. Two Windspeed anemometers were mounted at Baxter. One anemometer measured wind speed in the horizontal plane, while another measured wind speed in the vertical plane. JUS 2003 contained extensive wind data at the central business district of Oklahoma City, and three datasets were selected: Dugway Proving Ground sonic 13 (DPG_SuperPWID13), Los Alamos National Laboratory sonic green (LANL_sonicgreen), and Lawrence Livermore National Laboratory sonic H (LLNL_sonicH). All datasets in JUS 2003 were recorded using a 3D anemometer that captured simultaneously all wind velocity components at a frequency of 0.1s and a resolution of 0.01m/s. Figure 3 shows the velocity duration curves for Baxter and each dataset of JUS 2003.

Table 3 lists mean speed for each component V_v, V_w, V_u, and the resultant speed V of each dataset. In general, the mean speed of wind observed in the central business district of Oklahoma City is higher than the mean speed of wind observed on Caltech campus. LLNL_SonicH is mounted at 83.2m above ground, the highest elevations among all three anemometers of JUS 2003 datasets, and yields the highest mean wind speed V.

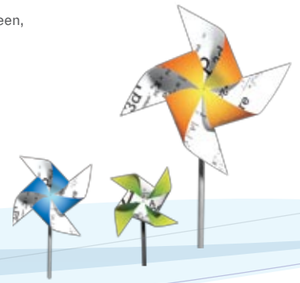

			Mean Speed (m/s)			
	Air Density (kg/m³)	Observation Period (sec)	V_u	V_v	V_w	V
DPG Sonic 13	1.29	592035.4	0.59	1.55	0.55	1.88
LANL SonicGreen	1.29	603122.2	1.16	0.57	0.81	1.74
LLNL SonicH	1.29	486092.3	1.78	3.19	0.66	4.10
Baxter	1.29	118529	0.5	0.5	0.2	0.7

Table 3. Wind conditions observed for 1) DPG Sonic13, 2) LANL SonicGreen, 3) LLNL SonicH, and 4) Baxter. Because air density was not measured at any location, it was assumed to be 1.29 kg/m³ , the standard air density. We integrate individual velocity duration curves over the total observation period to determine the mean speed of corresponding components.

Figure 4 shows the power duration curves of each of the individual velocity components and the resultant velocity for all four datasets. The area under each power duration curve is equivalent to the energy potential of the respective velocity component. The graphs demonstrate varying wind conditions at each location. At some locations, such as conditions observed by DPG Sonic 13, wind travels in one dominant direction, and the corresponding velocity component V_v provides the only meaningful source of wind energy extraction. However, at other locations, such as conditions observed by LANL Sonic Green and LLNL Sonic H, while wind still travel in one dominant direction, one or two other velocity components also have significant energy potentials. Therefore, at such locations extracting wind energy from only one direction would mean the loss of significant energy from other directions.

Datasets/Velocity Components	Total Energy (j/m²)	Average Power Flux – steady speed (watts/m²)	Average Power Flux – speed fluctuations (watts/m²)	Energy Pattern Factor	Special Energy Pattern Factor	Total Energy Pattern Factor
DPG Sonic13						
V_v	3810000	2.42	6.43	2.7	1.8	3.7
V	5340000	4.31	9.01	2.1	n/a	n/a
LANL SonicGreen						
V_s	2610000	0.99	4.32	4.3	3.4	7.7
V	4640000	3.41	7.69	2.3	n/a	n/a
LLNL SonicH	2320 0000	20.96	47.83	2.3	2.1	3.5
Baxter	35700000	44.55	73.48	1.7	n/a	n/a
Vertical Plane	59000	0.1	0.6	7.0	2.6	n/a
Horizontal Plane	120000	0.2	1.0	5.2	1.1	n/a

Table 4. Potential energy in wind conditions observed by DPG Sonic13, LANL SonicGreen, LLNL SonicH, and at Baxter

	No Fluctuations	Speed Fluctuations	Directional Fluctuations	Total Fluctuations
DPG Sonic13 - Power Output Analysis of V_v				
percentage of average annual household energy consumption provided by wind power	9.19%	24.37%	16.33%	34.16%
percentage of average monthly energy consumption of traffic signals provided by wind power	1.40%	3.70%	2.48%	5.19%
average time needed to charge a laptop battery (hr)	27.23	10.26	15.32	7.32
LANL SonicGreen - Power Output Analysis of V_s				
percentage of average annual household energy consumption provided by wind	3.77%	16.37%	12.92%	29.14%
average time needed to charge a laptop battery (hr)	66.36	15.27	19.36	8.58
amount of time one compact fluorescent light bulb can be powered by wind energy collected in day (hr)	2.17	9.43	7.44	16.78
LLNL SonicH - Power Output Analysis of V_v				
percentage of average annual household energy consumption provided by wind	79.41%	181.25%	168.81%	278.46%
percentage of average monthly energy consumption of a office building provided by wind	0.92%	2.10%	1.96%	3.23%
average time needed to charge a laptop battery (hr)	3.15	1.38	1.48	0.90

Table 5. **Power consumption vs. power output** analysis for each dataset using three of the following five models: Average energy capacity of laptop battery: 66Whr vs. power through a windswept area of 1m². Average power consumption of compact fluorescent light bulbs: 11watts vs. energy through a windswept area of 1m² in a day. Average energy used by US household per year: 8900kWh vs. energy through a windswept area of 38.5 m² in a year. Average monthly energy consumption of an office building: 63000 kWh vs. energy through a windswept area of 38.5 m² in a month. Average monthly energy consumption of traffic signals: 500 kWh vs energy through a windswept area of 4m². Each column indicates energy output under certain conditions, and each row analyzes a specific energy consumption model.

Table 4 lists total energy, average power flux, EPF, SEPF, and TEPF of the resultant velocity $\boldsymbol{V}$ and the dominant velocity component at each site. For example, in dataset of DPG Sonic13, power flux of $\boldsymbol{V_v}$ with steady speed is smaller by a factor of 2.7 (EPF) comparing to power flux of with speed fluctuations. EPF indicates that energy extracted from the wind can be potentially increased by a factor of 2.7 if wind speed fluctuations are captured. Power flux of $\boldsymbol{V_v}$ with steady speed is smaller by a factor of 1.8 (SEPF) comparing to power flux of $\boldsymbol{V}$ with steady speed. SEPF indicates that energy extracted from the wind can be potentially increased by a factor of 1.8 if the other two wind velocity components are captured. Finally, power flux of $\boldsymbol{V_v}$ with steady speed is smaller by a factor of 3.7 (TEPF) comparing to power flux of with fluctuating speed. TEPF simply indicates the energy extracted from wind can be potentially increased by a factor of 3.7 if both directional and speed fluctuations are captured. Similarly, for other datasets, each stage of power increase is characterized by respective factors of EPF, SEPF, and TEPF. Among the datasets, the site of LLNL SonicH offers the most promising location to extract significant wind energy. The site not only already provides considerable power flux from merely extracting wind with steady speed, but also has the potential to double or even triple its energy production by harvesting speed and directional fluctuations.

Table 5 analyzes power consumption models with potential energy output from each site. Average energy used by traffic signals in the central business district of Oklahoma City per month is 500kWh. If we assume four low speed wind turbines, each with a windswept area of 1m², are individually mounted on traffic poles at the intersection, then, as power analysis of DPG Sonic13 shows, wind power still provides an insignificant source of energy for traffic signals, even if all potential in fluctuations are captured. However, if one wind turbine with windswept area of 38.5 m² is mounted on the roof of Capital One building (83.2m above ground), power output analysis of LLNL SonicH shows that wind energy captured can power an average American household or even an office building. Other power consumptions analyses also illustrate that capturing wind speed fluctuations, directional fluctuations, or fluctuations in both areas can increase energy output by factors of EPF, SEPF, and TEPF respectively.

Limitation of the Study

Several limitations exist in this study. First, there are instrument limitations. Windspeed anemometer captures temporal speed fluctuations over a short duration of one second, while Taylor Precision anemometers average those speed fluctuations over a duration of one minute. The effects of changing frequency of wind speed data collection on EPF and SEPF has not been investigated. Secondly, the study is restricted by the approximations of power flux used in data analysis. Analytical expressions of power flux, EPF, SEPF, and TEPF approximate the theoretical expressions when the speed of individual components in concern approaches the speed of the resultant velocity vector, or $|V_v| \sim |V_{3d}|$. We analyze the wind velocity component in the dominant direction of travel to minimize deviations in approximated values from theoretical values. Further area of studies may investigate the degree of error in approximations.

Can wind be a viable source energy in urban environments?

Several important factors determine whether wind conditions at a specific location in an urban environment can provide a significant source of energy. Mean wind velocity is still the most important indicator for the magnitude of available energy potential. However, studies show that three other indicators - energy pattern factor (EPF), spatial energy pattern factor (SEPF), and total energy pattern factor (TEPF), also play an important role in judging the total energy potential available. Especially in urban environments where fluctuating wind prevails, data shows wind conditions at locations with relatively low speeds but high fluctuations can still provide a significant source of energy.

Three factors analyzed in this study, EPF, SEPF, TEPF, provide important indicators in determining which area of fluctuations are significant in a particular urban environment. Environments with high EPF and low SEPF indicate that wind has prevalent speed fluctuations but a dominant direction of flow. Therefore, turbines that capture these sudden gusts can maximize the wind energy extracted. On the other hand, environments with low EPF and high SEPF indicate that wind flows with a fairly steady speed but in no particular direction. Therefore, turbines that capture wind in all directions can maximize the wind energy extracted. For wind conditions in an urban environment, when one or more of these factors becomes non-negligible, the corresponding areas of fluctuations must be captured for wind to be a viable source of energy. While we do not show how to build such wind turbines, we hopefully provide the motivations for further wind turbine developments. Maybe in the future, individual buildings and homes installed with small wind turbines combined with solar panels and other renewable energy sources can eventually become energy independent, rendering electricity grids irrelevant and central power plants obsolete.

Further Reading

1. Allwine, K. J. and J. E. Flaherty (2006). Joint Urban 2003: Study Overview and Instrument Locations, Pacific Northwest National Laboratory and U.S. Department of Energy. Data retrieved from http://ju2003.pnl.gov/default.htm.
2. Gipe, Paul, and Richard Perez. Wind Energy Basics : A Guide to Small and Micro Wind Systems. New York, NY: Chelsea Green, 1999.
3. Golding, E. W. (1977). The Generation of Electricity by Wind Power. London, Halsted Press.
4. Handa, Kamal. Turbulence characteristics and Wind Energy Spectra. Tech.No. 2. Goteborg.

Acknowledgements

Fei Yang is a sophomore studying mechanical engineering. He would like to thank John for being a patient mentor and guiding him throughout the entire research. He would like to thank Madeline and Lydia for answering his questions. Also, he would like to thank Mike Tope for helping him set up an anemometer on Thomas radio tower, Susan Davis for kindly providing him access to the roof of Baxter, Rick Caney for helping him mount an anemometer on Baxter, and many others who made his project possible. Finally, he would like to thank Mr. and Mrs. Daily for generously supporting his SURF project.

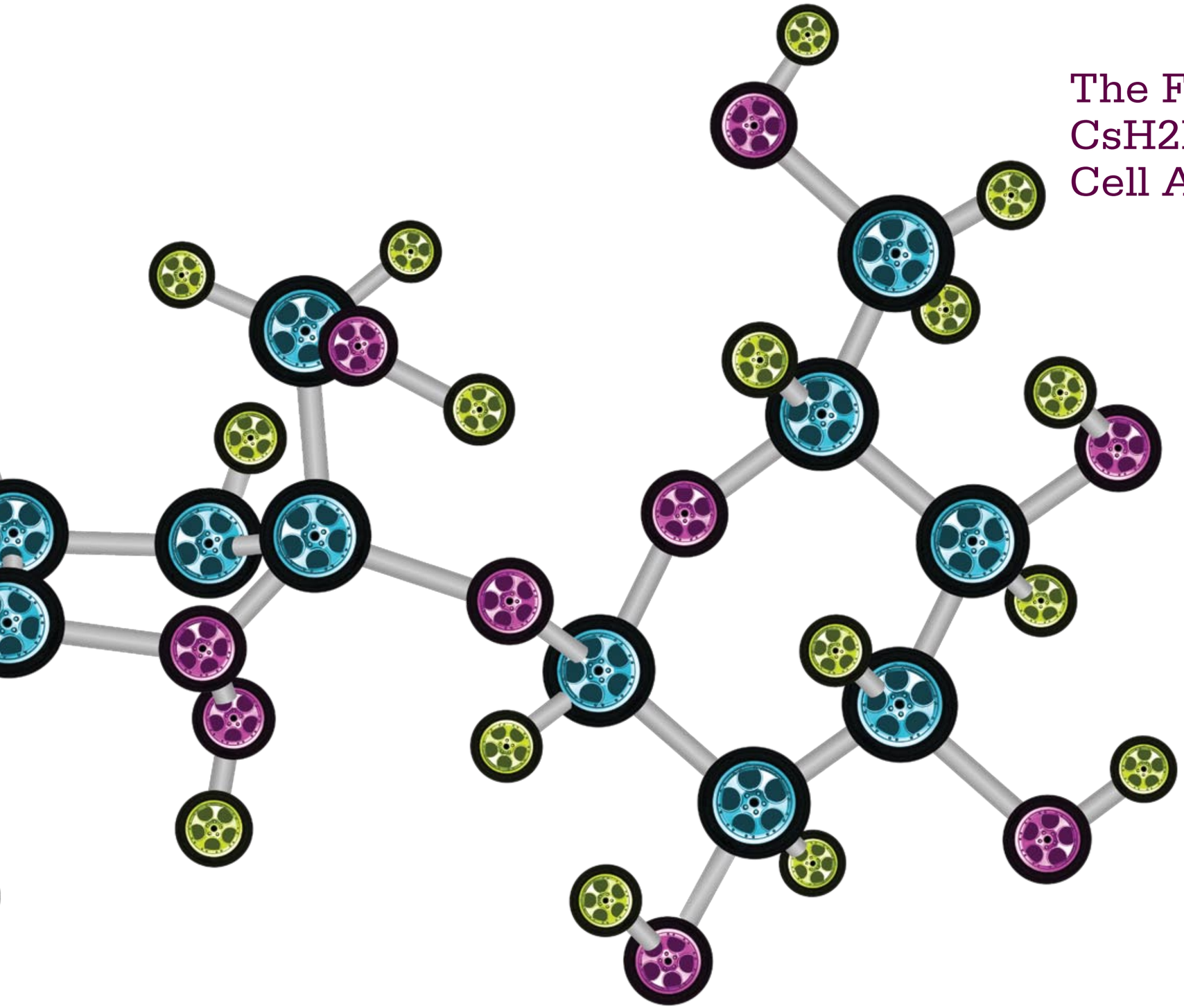

The Fabrication of Nanoparticle CsH2PO4 Electrolyte for Fuel Cell Applications

Helen Telila, Tewodros Mamo and Raul Hernandez Sanchez.

Take a moment to think about how automobiles are powered these days: most are either gasoline-powered or battery-gas hybrids. However, gasoline-powered cars emit CO2, CO, and other environmentally unfriendly gases. In comparison, fuel cell-powered cars that use hydrogen fuels emit water vapor and little to no CO2/CO waste. Currently, Honda has marketed the FCX Clarity model which uses Polymer Electrolyte Membrane Fuel Cells (PEMFCs). However, PEMFCs require platinum catalysts, which are precious and costly. Another type of fuel cell called Solid Acid Fuel Cell (SAFC) has the potential to provide this clean energy technology much more economically and efficiently than PEMFCs. In order to accomplish this, first the efficiency of SAFCs need to be improved. Thus, the focus of this research is to fabricate nanoscale CsH2PO4 (CDP) particles that will improve the efficiency of CDP based SAFCs.

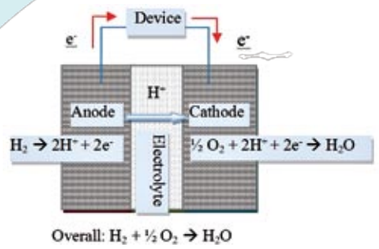

Figure 1. A schematic of a fuel cell based on a proton conducting electrolyte.

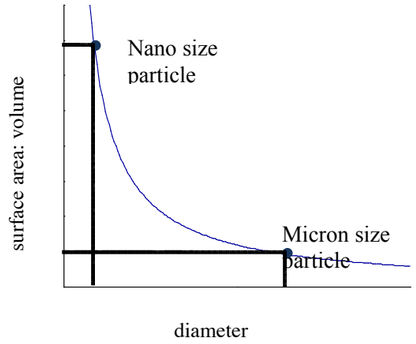

Figure 2. A schematic of surface area to volume ratio vs. diameter for a sphere like particle..

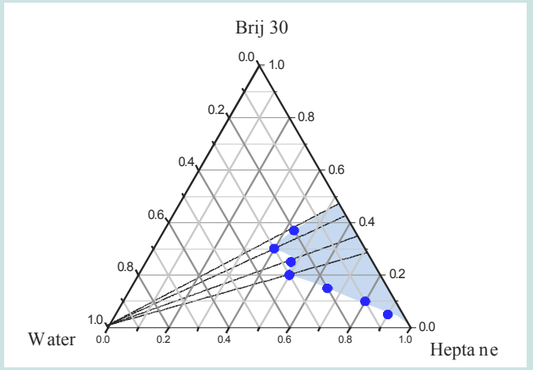

Figure 3 Ternary phase diagram of the system Water / Brij 30 / Heptane.

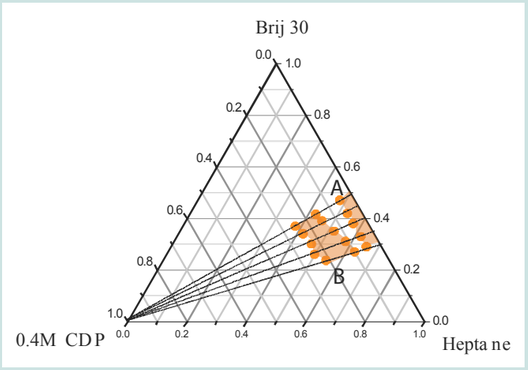

Figure 4. Ternary phase diagram of the system: 0.2M CDP / Brij 30 / Heptane. The shaded region A corresponds to a microemulsion, however it is ambiguous whether the second shaded region, B, is a microemulsion or not.

Solid Acid Fuel Cell Basics

A fuel cell is a device that directly converts chemical energy to electrical energy without using a combustion reaction. Fuel cells are more efficient than combustion engines as they are not limited by the Carnot efficiency. A fuel cell consists of an electrocatalytically active anode and cathode separated by an electrolyte. The electrolyte allows the passage of ions while preventing the flow of electrons and molecules between the cathode and the anode. Ideally, the electrolyte is impermeable to gases and hence it prevents combustion reactions that could otherwise occur between the fuel and the oxidant. Instead, half-cell reactions take place at the electrodes and produce ions that pass through the electrolyte, and electrons that flow through an external circuit (Fig. 1).

In a fuel cell, the electrolyte determines the type of reaction that occurs at the electrodes and hence fuel cells are classified based on the electrolyte employed. PEMFCs have a polymer membrane electrolyte that needs to be fully hydrated in order to be conductive to protons. The protons need to attach to water molecules in order to pass through the membrane. As a result, the operating temperature needs to be below 100 °C, and it is costly to keep PEMFCs at lower temperatures. Conversely, SAFCs based on CsH2PO4 (CDP) electrolytes have shown promising results in the intermediate temperature region (~200 - 300°C); they have demonstrated power densities as high as 415 mW/cm2 (ref. 1). The proton conduction in SAFCs takes place under anhydrous conditions - the protons are transported through the electrolyte without the aid of water molecules. These properties of SAFCs make them feasible for intermediate temperature applications, such as car engines. The performance of SAFCs, however, is limited by the activation overpotential at the electrodes (ref. 2); more work needs to be done to improve their efficiency before they can be marketed. Once SAFC based technologies are fully developed, they can potentially replace PEMFCs.

The electrochemical reactions of a fuel cell take place at the triple-phase boundary sites; these are the sites where the catalyst, the electrolyte and the gas intersect. It is expected that increasing the number of triple-phase boundary sites increases the amount of current that passes through the electrode and hence increases the performance of the fuel cell. To increase the triple-phase boundary sites, nano-sized electrolyte and catalyst particles need to be employed in the electrode composite. A schematic of surface area to volume ratio vs. diameter shows that as the diameter of a particle decreases, its surface area to volume ratio increases, and vice versa (Fig. 2). Higher surface area to volume ratio entails higher number of triple-phase boundary sites. If both the catalyst and the electrolyte have small diameters, then there will be more surface area and hence more reaction sites in the electrode composite. Therefore, the fabrication of nano-CDP would provide increased surface area of electrolyte and a higher number of triple phase boundary sites at which electrocatalysis can occur.

In this project, nano-CDP was fabricated using a microemulsion mediated synthesis with a non-ionic surfactant (Brij(R)30), n-heptane and CDP (aq). The prepared products were characterized by Scanning Electron Microscopy (SEM), solid state Nuclear Magnetic Resonance (NMR) and X-Ray Diffraction (XRD). Furthermore, different CDP concentrations were used to determine the phase diagram for the ternary system (Brij30/n-heptane/CDP).

Microemulsion Mediated Synthesis

Ideally, nano-sized CDP particles can be synthesized using a method based on water-in-oil (W/O) microemulsions. Microemulsions are thermodynamically stable, clear and isotropic solutions composed of water (polar phase), oil (non-polar phase) and a surfactant. Surfactants have hydrophobic tails that interact with non-polar solvents and hydrophilic heads that interact with polar molecules, such as water. When surfactants are added to a mixture of oil and water, they assemble themselves into different structures depending on the relative compositions of the three components. The different structures lead to different phases, indicated by ternary phase diagrams with the three components at the apex of an equilateral triangle. One of these phases is W/O microemulsion in which the surfactant traps nano-sized water droplets, creating inverted micelles (Fig. 3). A W/O microemulsion forms close to the oil apex region of a water/oil/surfactant system. To synthesize CDP nanoparticles, an aqueous solution of CDP was used as the polar phase; thus, when the inverted micelles are formed, the CDP particles will be trapped inside them.

Once aqueous CDP is incorporated in the nano-sized inverted micelles, various methods can be employed to precipitate the CDP particles. In the first of these methods, two microemulsions with the same composition were mixed to get CDP nanoparticles. A CDP microemulsion composed of aqueous CDP, heptane and Brij 30 was mixed with a methanol (MeOH) microemulsion composed of MeOH, heptane and Brij 30. The MeOH molecules interact with the water molecules, which results in less interaction between the CDP and the water molecules, and hence the CDP particles precipitate out. The surfactant of choice, Brij 30, is a non-ionic surfactant and thus expected to be free from any ionic contamination; however, it was found to contain some so-

Table 1. Weight percent of each microemulsion used to precipitate the CDP particles. The concentrations correspond to Figure 4B.smaller the particle is the larger the surface area for a fix volume of particles.

CDP microemulsion	MeOH microemulsion
20 wt% 0.2M aq. CDP	20 wt% MeOH
30 wt% Brij 30	30 wt% Brij 30
50 wt% Heptane	50 wt% Heptane

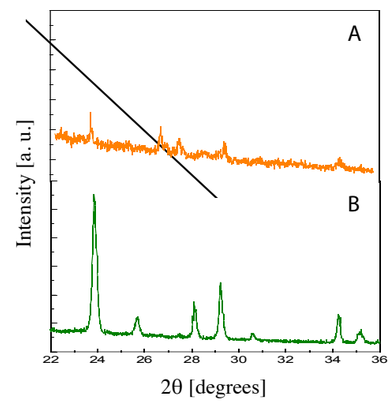

Figure 5. X-ray diffraction patterns of (A) precipitates collected from 1:5 0.2M CDP to methanol microemulsion and (B) bulk CDP.

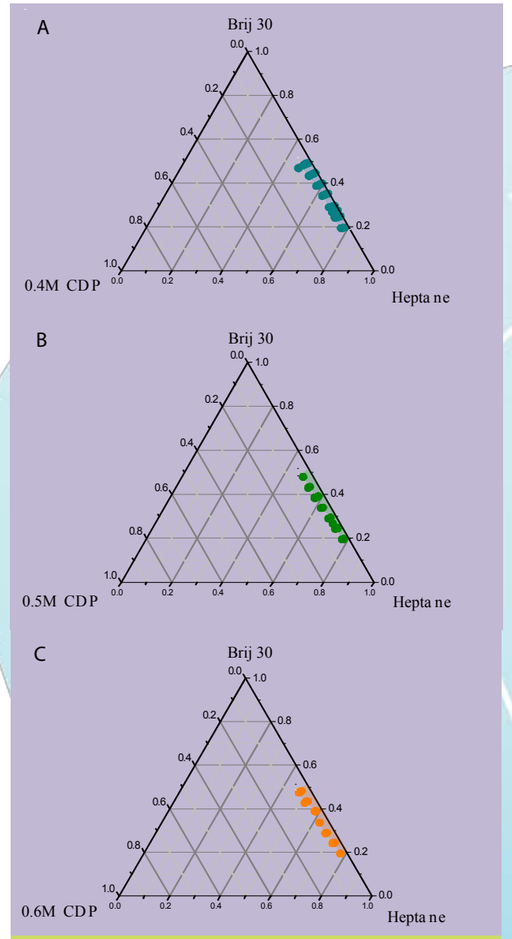

Figure 6. Ternary phase diagrams of the (A) 0.4, (B) 0.5 and (C) 0.6M CDP / Brij 30 / Heptane systems.

Table 2. Weight percent of each of the components in the 0.4M CDP and MeOH microemulsions. Concentrations relevant to Figure 6A.

CDP microemulsion	MeOH microemulsion
3.2 wt% 0.4M aq. CDP	3.2 wt% MeOH
26.6 wt% Brij 30	26.6 wt% Brij 30
70.2 wt% Heptane	70.2 wt% Heptane

dium impurities. Tracing back the production of Brij 30 revealed the source of sodium contamination – sodium is used as one of the reagents in the industrial production of Brij 30. The sodium contamination was further confirmed by 23Na-NMR of Brij 30. Later, Brij 30 was purified using a method based on dialysis; the details will be discussed elsewhere.

Synthesis Based on Dilute CDP Solution

Submicron sized CDP particles were synthesized using a 0.2M CDP/Brij 30/Heptane system (Fig. 4). In the phase diagram, there are two clear (shaded) regions; the "unknown" region, Fig. 4B, is further down the microemulsion region; thus, it may or may not be a microemulsion. The CDP to Brij 30 ratio of the "unknown" region is higher than that of the microemulsion region; thus, it is expected to result in less sodium contamination if unpurified Brij 30 is to be used.

To precipitate the CDP particles, a MeOH microemulsion of the same composition as the CDP microemulsion is used. Table 1 shows the selected compositions for both microemulsions; these compositions lay in region B and this region was picked because the sodium contamination needed to be minimized by increasing the ratio of CDP to Brij 30. Here the CDP and MeOH microemulsions were mixed in a one to five weight ratio to get a high yield. The calculated CDP particle size for the given composition is on the nano scale; however, the actual particle size is on the micro scale. CDP is hygroscopic and hence the particles quickly absorb water from the atmosphere resulting in particle growth. Furthermore, the XRD patterns of the CDP precipitates do not match that of bulk CDP; the extra peaks indicate that there is sodium contamination in the final product (Fig. 5). From these results, it was concluded that pure nano-sized CDP particles cannot be synthesized using this composition unless pure Brij 30 is used.

Synthesis Based on more Concentrated CDP Solution

In order to lower the amount of sodium impurity in the CDP particles, it was necessary to boost the ratio of CDP to Brij 30. To do this, the concentration of aqueous CDP in the microemulsions was increased; initially a 0.4M CDP/Brij 30/Heptane system was used, but later 0.5M CDP/Brij 30/Heptane and 0.6M CDP/Brij 30/Heptane systems were studied (Fig. 6). Unlike the phase diagram of the 0.2M CDP/Brij 30/Heptane system, the phase diagrams of the 0.4, 0.5 and 0.6M CDP/Brij 30/Heptane systems show only one clear region. To increase the CDP to Brij 30 ratio further, higher weight percents of the CDP to MeOH microemulsion were used. Thus far, a 1:5 mass ratio of CDP to MeOH microemulsion was used. Increasing this ratio would decrease the amount of Brij 30 in the system and hence the CDP to Brij 30 ratio would increase; thus the sodium contamination would decrease. Up to 5:1 ratios of CDP to MeOH microemulsions were investigated and the resulting samples were characterized by SEM and XRD.

Using the composition in Table 2, different ratios of CDP to MeOH were used to synthesize nano-sized CDP. The XRD patterns of the resulting precipitates from the 1:1 and 1:5 (0.4M CDP to MeOH) ratios show that the precipitates from the 1:1 ratio give a clean XRD pattern (Fig. 7A); however the 1:5 ratio shows some extra peaks (Fig. 7B) that do not match the peaks of bulk CDP (Fig. 7C). This shows that the ratio of CDP to MeOH needs to be close to 1:1 to get pure nano-CDP.

Synthesis with and without the Methanol Microemulsion

The SEM image of the precipitates collected from mixing CDP and MeOH microemulsion in varies ratios show that the particles are growing (Fig. 8). The calculated CDP particle size for the composition of Table 2 is ~0.82 nm, but the SEM images show micron sized CDP particles. CDP is very hygroscopic and hence particle growth could take place before or after the synthesis. To lower the particle growth, the CDP precipitates were collected by drying the CDP microemulsion without using the

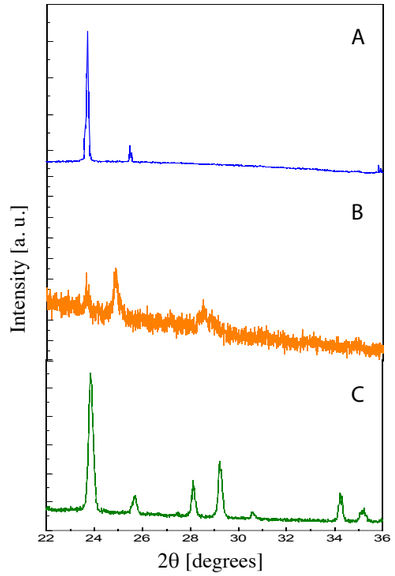

Figure 7. X-ray diffraction patters of (A) the precipitates collected from the 1:1 and (B) 1:5 microemulsions (0.4M CDP : methanol microemlusion) and (C) bulk CDP.

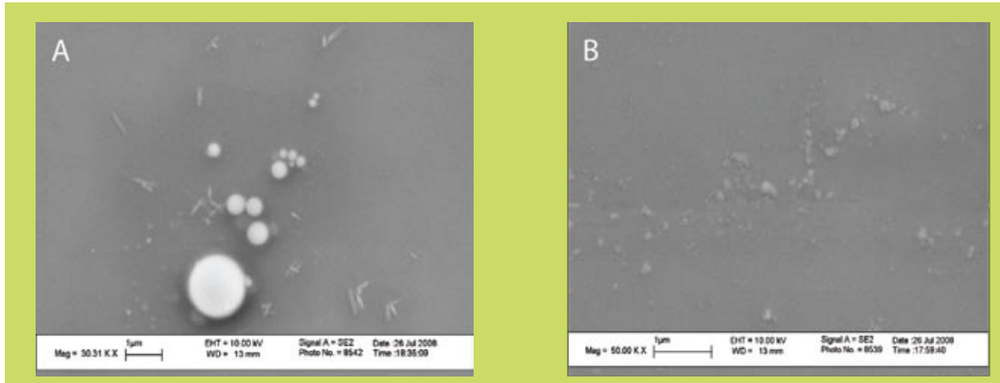

Figure 8. SEM images of the precipitates collected from (A) the 1:2 and (B) 1:4 ratios of 0.4M CDP to MeOH microemulsions.

MeOH microemulsion. This was first done by drying the CDP microemulsion in a desiccator followed by a nitrogen flow. The SEM images of the resulting CDP particles show that it is possible to recover the nanoparticles without using the MeOH microemulsion (Fig. 9). Avoiding the use of the MeOH microemulsion lowers the contamination level as well as the particle growth. However, the particle sizes recovered by drying the CDP microemulsion are far from the calculated particle size. The particle sizes are on the order of 100 nm. This is believed to be due to the hygroscopic property of CDP.

Freeze Dried CDP Microemulsion

In order to dry the CDP microemulsion with minimal particle growth, other approaches were followed. Thus far, freeze drying the microemulsion for several hours has been promising. During the freeze drying process, it is expected that the water molecules will be removed from the system while encapsulated CDP nanoparticles are left behind in the frozen state. Keeping the system frozen prevents the solution from getting outside the microemulsion region. During this process, water and heptane are removed from the system and thus it is expected to prevent particle growth. However, the resulting SEM images of the freeze dried sample show that the particles are growing (Fig. 10). Comparing these images to those of Fig. 9, the particles' size is slightly smaller and evenly distributed. At this point, it is not evident whether particle growth is taking place before or after the freeze drying process.

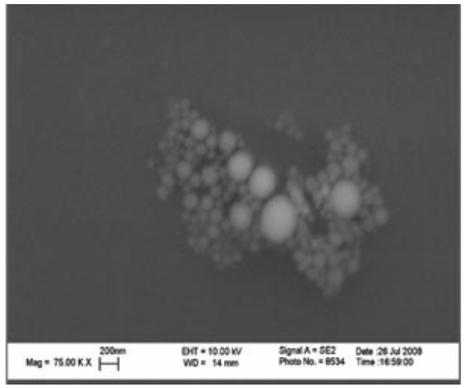

Figure 9. SEM image of CDP particles collected by drying the 0.4M CDP microemulsion in a desiccator.

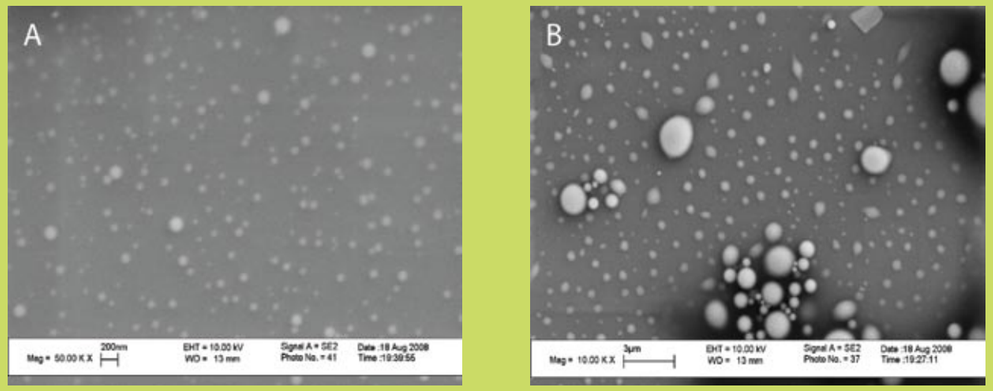

Figure 10. SEM images of CDP particles after 16 hours of freeze drying. (A) Scale down to 200nm and (B) scale down to 3um.

Conclusion

In summary, it was possible to fabricate nano-sized CDP particles by freeze drying a CDP microemulsion made of 0.4M CDP/Heptane/Brij 30 system. This method is preferred to using two microemulsions where methanol forms the aqueous phase of the second microemulsion. Avoiding the use of a second microemulsion resulted in less Brij 30 in the system and hence less sodium contamination. Additionally, smaller particle size was obtained in the case of freeze drying. The challenge with the microemulsion mediated synthesis of CDP has been the recovery of nano-sized particles without altering their size. This requires the removal of water from the inverse micelles without changing the size of the precipitating CDP particles. The freeze drying approach has been promising in achieving this goal. However, the SEM images of the freeze dried samples show particle growth indicating that there is some residual water remaining in the system. Future work should focus on making the freeze drying process more efficient.

Acknowledgements

Helen Telila is a senior at Mt. Holyoke majoring in Chemical Physics. Tewodros Mamo is a junior at University of Waterloo majoring in Nanotechnology Engineering. Raul Hernandez-Sanchez is a fourth-year student at ITESM Campus Monterrey majoring in Chemistry. They would like to thank Prof. Sossina Haile, Dr. Ali Samarat, Mary Louie, the Haile Group and the Caltech SFP office. This work was funded by the Gordon and Betty Moore Foundation, through its support of the Caltech Center for Sustainable Energy Research.

References

1. T. Uda and S. M. Haile, "Thin-Membrane Solid-Acid Fuel Cells," Electrochemical and Solid-State Letters 8 (5), A245-A246 (2005).
2. S. M. Haile, C. R. I. Chisholm, K. Sasaki, D. A. Boysen and T. Uda, "Solid Acid Proton Conductors: From Laboratory Curiosities to Fuel Cell Electrolytes," Faraday Discussions 134, 17-39 (2007).

Further Readings

1. D.G. Shchukin and G.B. Sukhorukov, "Nanoparticle Synthesis in Engineered Organic Nanoscale Reactors," Advanced Materials 16, 671-681 (2004).
2. S. M. Haile, "Fuel Cell Materials and Components," Acta. Met. 51, 5981-6000 (2003).
3. C. Destree and J.B. Nagy, "Mechanism of Formation of Inorganic and Organic Nanoparticles from Microemulsions," Advances in Colloid and Interface Science 123-126, 353-367 (2006).
4. V. Marciano, A. Minore and V. T. Liveri, "A Simple Method to Prepare Solid Nanoparticles of Water-Soluble Salts Using Water-in-Oil Microemulsions," Colloid Polym Sci 278, 250-252 (2000).

"Aniket Schneider graduated from MIT in 2007 with a B.S. in biology. He is currently working in the biotechnology industry while applying to medical school. Aniket and the MIT Undergraduate Research Journal have kindly allowed CURJ to reprint this article for your reading pleasure. We hope you enjoy this glimpse of undergraduate research from MIT!"

Emerging Technologies for Influenza Vaccination

Aniket Schneider

Abstract

Mounting concerns about the pandemic potential of H5N1 avian influenza make the development of more effective vaccines an urgent need. Because of the high pathogenicity of the H5N1 viruses, conventional vaccines cannot be produced against these strains. New vaccines based on reverse genetics will soon become licensed, but suffer from limitations in production capacity. New, more robust techniques, however, are still in the early stages of development. This review discusses the current status of influenza vaccination technology and the drawbacks and benefits of various emerging techniques.

Introduction

The influenza virus spreads across the world in seasonal epidemics, causing approximately 250,000 to 500,000 deaths per year. While most people recover within one to two weeks without medical attention, the very young, the elderly, and people suffering from various co-morbidities experience more serious complications[1]. On rare occasions, influenza strains arise to which humans have no innate immunity. These strains have the potential to create pandemics such as the Spanish Flu pandemic in 1918 which killed over 40 million people[2].

The classification of a strain of influenza virus depends on the various antigenic proteins expressed by the virus. Differences between the nucleoprotein and matrix protein of the virus are used to classify virus strains into three broad categories, types A, B and C, with type A being the most virulent in humans. Type A strains are further subdivided by differences in their surface glycoproteins, hemagglutinin (HA) and neuraminidase (NA). These two proteins, particularly hemagglutinin, provide the major targets for the host immune response[3]. Currently, the H1N1 (hemagglutinin 1, neuraminidase 1) and H3N2 strains of influenza A circulate most widely in humans[1].

Recently, however, a new strain of influenza, with many of the characteristics of a pandemic virus, has been discovered in birds. This virus, classified as an H5N1 strain of influenza A, has a very high pathogenicity, and of the 291 confirmed cases of infection to date, 172 (59%) have resulted in the death of the patient[4]. Luckily, the virus cannot yet be transmitted from human to human, but health care officials are concerned that it may reassort with another influenza strain and become a major pandemic threat[5].

Apart from its high pathogenicity and mortality rates, H5N1 avian flu has several features that make it a particularly potent pandemic threat. Because of the strain's novel H5 surface antigen, humans have no preexisting immunity to the virus. Additionally, there are no known H5N1 strains with low pathogenicity from which to produce a vaccine. Finally, due to extensive use of antiviral drugs to control the spread of illness in poultry during a 1997 outbreak of H5N1 in Hong Kong, much of the H5N1 virus in circulation is already resistant to one of the major influenza antiviral drug types, adamantane[6]. Because of these factors, development of a vaccine against H5N1 avian flu has become a high priority.

Conventional Vaccines

The standard method for creation of influenza vaccines involves growing a virus in embryonated chicken eggs. Allantoic fluids of the eggs are harvested and the virus is purified out, after which it can be injected directly, and function as a live virus vaccine, or it can be chemically inactivated, and function as an inactivated whole virus or inactivated subvirion vaccine[3]. However, the high pathogenicity of H5N1 strains presents a challenge to this traditional approach of vaccine production in an egg: not only does the virus present an unusually great danger to the people working on the vaccine, requiring a higher biosafety level than is present in most production plants, but it also infects the eggs so effectively that it kills the eggs before the virus reaches a sufficiently high concentration for harvesting[5].

Substances called adjuvants can greatly increase the potency of vaccines administered at low doses, a technique that is especially useful when very little vaccine is available[7]. Many types of compounds can be used as adjuvants, but the ones most commonly effective with influenza vaccines are an aluminum salt called alum, and a proprietary emulsion of squalene called MF59[7, 8]. The use of both types of adjuvants in humans is currently being tested in large-scale clinical trials in the US, and MF59 is already in use in European vaccines[7]. Despite their promise, though, adjuvants have not solved the problem of creating a pandemic flu vaccine, and United States regulatory agencies have been slow to approve their use[7].

Attempts to use related low pathogenic avian influenza (LPAI) strains to create vaccines against H5N1 have met with very limited success[9,10]. These vaccines achieved acceptable immunogenicity when augmented by the use of an adjuvant, demonstrating that adjuvants increase the cross-reactivity of the antibodies induced by a vaccine. Despite their low pathogenicity, however, these strains grew poorly in chicken eggs[10]. This type of vaccine avoids most licensing barriers by making use of previously licensed technology, but production limitations make these vaccines suitable only for high-risk patients.

Reverse Genetics

The most promising body of research into vaccine production involves a technique called reverse genetics, which allows manipulation of the virus genome in cell culture[11-15]. A set of plasmids encoding the entire virus genome is transfected into a eukaryotic cell line, allowing the cells to produce entire virus particles without having been infected[15]. Because of the ease with which plasmid DNA can be modified, this general approach allows controlled manipulation of the features of an influenza strain, and can be used to produce desired characteristics like low pathogenicity and specific surface antigens.

Research has focused on two classes of vaccines produced with reverse genetics, whole virion and subvirion vaccines. In whole virion vaccines the inactivation process preserves the overall structure of the virus particle. Subvirion vaccines, on the other hand, include only specific purified protein subunits. Immunogenicity of whole virion vaccines generally exceeds that of subvirion vaccines[16], making them good candidates for pandemic flu vaccines.

Generally, both types of vaccines are derived from two influenza strains, a pathogenic strain and an attenuated strain. The pathogenic strain supplies genes for the surface glycoproteins, allowing the vaccine to generate a specific immune response against the original strain. Genetic material from the attenuated strain reduces the pathogenicity of the recombinant virus, allowing it to grow efficiently in eggs. Additionally, in the case of H5N1, the H5 antigen actually causes some of the high pathogenicity of the strain, so the sequence of the H5 HA gene must be modified to reduce this effect[3].

Treanor and colleagues developed an inactivated subvirion vaccine as a preliminary step toward a whole virion vaccine[13]. Using reverse genetics, they replaced the surface antigens of a common vaccine platform virus with H5N1 surface antigens, and modified the H5 HA gene to reduce pathogenicity, allowing efficient growth of the seed virus in eggs[13]. The resulting virus was purified out of the eggs and disrupted into its component proteins using a detergent, after which the H5 HA and N1 NA proteins were purified out and administered to patients

without adjuvant[13]. While this vaccine was only marginally effective at high doses (two doses of 90 ug induced protective antibody levels in only 58% of patients[13]), use of an adjuvant could potentially increase its effectiveness.

Meanwhile, results of early clinical trials of an inactivated whole virion vaccine have shown promise. Lin and colleagues have created and tested a vaccine derived from a highly pathogenic H5N1 strain and an attenuated H1N1 strain, again with modifications to the H5 HA protein to reduce its pathogenicity[12]. This vaccine was prepared in the conventional way and inactivated using formalin[12], a chemical which disables the virus but preserves its structure. The vaccine, administered with an aluminum-based adjuvant, induced protective levels of antibody in around 80% of patients with a dose of only 10 ug[12]. The trials were conducted in China, however, and approval of this vaccine by foreign regulatory agencies will have to wait for larger scale trials under their jurisdiction.

Novel Alternative Approaches

Reverse genetics-based vaccines rely on well-established technology and tested techniques, and require no changes in the existing vaccine production infrastructure. There are disadvantages, however, to the conventional method. Drug companies base their production capacity on yearly sales, so there is no incentive for them to build the capacity for a pandemic response that may or may not come. The existing limited production capacity cannot be used to stockpile vaccine, because an emerging pandemic strain is likely to have mutated from the original vaccine targets. Finally, practical matters like egg supply and biosafety level requirements place additional limitations on vaccine production.

A number of new ideas are being explored in order to circumvent the weaknesses in conventional and reverse genetics-based vaccines. Increasing production capacity is one important priority, but others include creating broader-spectrum vaccines, increasing the effectiveness of small vaccine doses, and decreasing the lag time between identification of a strain and production of the vaccine. Most of these techniques are still under development, and have not yet undergone clinical trials in humans. Additionally, because they involve developing completely new technology, the licensure process for these vaccines will be longer. Nonetheless, they offer great potential for improving the effectiveness of future vaccines.

One idea is to simplify the manufacturing process by using recombinantly expressed HA protein alone as a vaccine. The gene for H5 HA is transfected into and expressed in cultured cells, which can then be induced to overexpress the H5 antigen[17]. The resulting vaccine is similar to an inactivated subvirion vaccine, but does not require the cumbersome egg-based system of production. In humans, this vaccine works only at high (90 ug) doses and only in roughly 50% of patients[17], but perhaps with the addition of an adjuvant to increase immunogenicity it could become a viable option.

Other researchers, attempting to broaden their range of protection, have created a vaccine which induces antibodies against the virus matrix protein, M2, which is conserved in all influenza A strains but is normally not immunogenic. The technique involves attaching M2e, the external portion of the M2 protein, to the hepatitis B virus core, which greatly increases its immunogenicity[18]. With the use of various adjuvants and with several copies of the M2e domain per particle, this vaccine successfully conferred protective immunity to an influenza A strain in mice, though the mechanism by which antibody production was induced is not well characterized[18]. This vaccine is still in the early testing stages, but it shows great promise since it would allow stockpiling of vaccine in advance of a pandemic outbreak, as well as immunization against a wide range of influenza strains with a single vaccine.

A very new type of vaccine using an adenovirus as a vector also circumvents many of the problems with conventional influenza vaccines, this time by allowing the host organism's body to do much of the manufacturing work. In this type of vaccine, a replication-defective adenovirus strain is modified to carry an antigen, in this case H5 HA. When the virus infects the host organism, the infected cells start producing large quantities of the antigen instead of producing new virus particles. Additionally, certain strains of adenovirus preferentially infect human antigen-presenting cells, which would amplify the immune response and allows use of a smaller vaccine dose[19]. Adenovirus vector-based vaccines have been tested in mouse and chicken model systems, and they confer protective immunity even against antigenically distinct flu strains, provided that they carry the H5 antigen[19, 20].

Adenovirus vector-based methods have been used in over 100 clinical trials for other purposes, so the technology is well understood[20]. Additionally, Gao and colleagues managed to move from virus sequence to vaccine production in just 36 days, which would facilitate fast response in case of a pandemic[20]. Finally, the vaccine can be produced efficiently in an egg-free system[19, 20]. Unfortunately, this type of vaccine is quite far from being licensed for use, at least in the United States. For now, having been proven in chickens, adenovirus vector-based vaccines may at least be useful for controlling the rampant spread of avian flu in poultry[20].

Conclusions

The FDA recently awarded the first US license for a vaccine against avian flu in humans to Sanofi-Pasteur for an inactivated subvirion vaccine[13, 21]. While this step will greatly enhance the country's ability to respond effectively to an H5N1 flu outbreak, it does not solve many of the systemic issues in conventional vaccine technology. Conventional vaccines such as this one, even those modified with reverse genetics, still suffer from production bottlenecks and shortages, as well as having relatively slow response times when facing a potential pandemic. Thanks to intensive research in recent years, a great many options for new types of vaccines now exist, but the most robust, cheap, and effective vaccines are still under development.

At the moment most governments, lacking a suitable vaccine to invest in, are stockpiling influenza antiviral drugs as their backup plan. H5N1 flu, however, has already developed considerable resistance to the adamantane class of drugs[6, 19], and recently various influenza strains are exhibiting resistance to oseltamivir[22, 23], one of the other two major classes of flu antiviral drugs. This development only serves to underscore the critical importance of continuing vaccine research.

References

1. WHO. Influenza Fact Sheet. http://www.who.int/mediacentre/factsheets/fs211/en/ April 18, 2007.

2. Johnson NP, Mueller J. Updating the accounts: global mortality of the 1918-1920 "Spanish" influenza pandemic. Bull Hist Med 2002; 76:105- 115.

3. Horimoto T, Kawaoka Y. Strategies for developing vaccines against H5N1 influenza A viruses. Trends Mol Med 2006; 12:506-514.

4. WHO. Cumulative Number of Confirmed Human Cases of Avian Influenza A/(H5N1) Reported to WHO. http://www.who.int/csr/disease/avian_influenza/country/cases_table_2007_04_11/en/index.html April 18, 2007.

5. Stohr K, Esveld M. Public health. Will vaccines be available for the next influenza pandemic? Science 2004; 306:2195-2196.

6. Li KS, Guan Y, Wang J et al. Genesis of a highly pathogenic and poten- tially pandemic H5N1 influenza virus in eastern Asia. Nature 2004; 430:209-213.

7. Wadman M. Race is on for flu vaccine. Nature 2005; 438:23.

8. Martin JT. Development of an adjuvant to enhance the immune response to influenza vaccine in the elderly. Biologicals 1997; 25:209- 213.

9. Nicholson KG, Colegate AE, Podda A et al. Safety and antigenicity of non-adjuvanted and MF59-adjuvanted influenza A/Duck/Singapore/97 (H5N3) vaccine: a randomised trial of two potential vaccines against H5N1 influenza. Lancet 2001; 357:1937-1943.

10. Stephenson I, Bugarini R, Nicholson KG et al. Cross-reactivity to highly pathogenic avian influenza H5N1 viruses after vaccination with nonad- juvanted and MF59-adjuvanted influenza A/Duck/Singapore/97 (H5N3) vaccine: a potential priming strategy. J Infect Dis 2005; 191:1210-1215.

11. Li S, Liu C, Klimov A et al. Recombinant influenza A virus vaccines for the pathogenic human A/Hong Kong/97 (H5N1) viruses. J Infect Dis 1999; 179:1132-1138.

12. Lin J, Zhang J, Dong X et al. Safety and immunogenicity of an inactivated adjuvanted whole-virion influenza A (H5N1) vaccine: a phase I randomised controlled trial. Lancet 2006; 368:991-997.

13. Treanor JJ, Campbell JD, Zangwill KM et al. Safety and immunogenicity of an inactivated subvirion influenza A (H5N1) vaccine. N Engl J Med 2006; 354:1343-1351.

14. Webby RJ, Perez DR, Coleman JS et al. Responsiveness to a pandemic alert: use of reverse genetics for rapid development of influenza vac- cines. Lancet 2004; 363:1099-1103.

15. Neumann G, Watanabe T, Ito H et al. Generation of influenza A viruses entirely from cloned cDNAs. Proc Natl Acad Sci U S A 1999; 96:9345- 9350.

16. Subbarao K, Luke C. H5N1 Viruses and Vaccines. PLoS Pathog 2007; 3: e40.

17. Treanor JJ, Wilkinson BE, Masseoud F et al. Safety and immunogenicity of a recombinant hemagglutinin vaccine for H5 influenza in humans. Vaccine 2001; 19:1732-1737.

18. De Filette M, Min Jou W, Birkett A et al. Universal influenza A vaccine: optimization of M2-based constructs. Virology 2005; 337:149-161

19. Hoelscher MA, Garg S, Bangari DS et al. Development of adenoviral- vector-based pandemic influenza vaccine against antigenically distinct human H5N1 strains in mice. Lancet 2006; 367:475-481.

20. Gao W, Soloff A, Lu X et al. Protection of Mice and Poultry from Lethal H5N1 Avian Influenza Virus through Adenovirus-Based Immunization. Journal of Virology 2006; 80:1959-1964.

21. Sanofi-Pasteur I. FDA Licenses First U.S. Vaccine for Humans Against Avian Influenza. http://en.sanofi-aventis.com/Images/20070417_h5n1_fda_en_tcm24-16537.pdf April 20, 2007.

22. de Jong MD, Tran TT, Truong HK et al. Oseltamivir resistance dur- ing treatment of influenza A (H5N1) infection. N Engl J Med 2005; 353:2667-2672.

23. Le QM, Kiso M, Someya K et al. Avian flu: isolation of drug-resistant H5N1 virus. Nature 2005; 437:1108.